

A SYMMETRIZED PARAMETRIC FINITE ELEMENT METHOD FOR ANISOTROPIC SURFACE DIFFUSION II. THREE DIMENSIONS

WEIZHU BAO* AND YIFEI LI†

Abstract. For the evolution of a closed surface under anisotropic surface diffusion with a general anisotropic surface energy $\gamma(\mathbf{n})$ in three dimensions (3D), where \mathbf{n} is the unit outward normal vector, by introducing a novel symmetric positive definite surface energy matrix $\mathbf{Z}_k(\mathbf{n})$ depending on a stabilizing function $k(\mathbf{n})$ and the Cahn-Hoffman ξ -vector, we present a new symmetrized variational formulation for anisotropic surface diffusion with weakly or strongly anisotropic surface energy, which preserves two important structures including volume conservation and energy dissipation. Then we propose a structural-preserving parametric finite element method (SP-PFEM) to discretize the symmetrized variational problem, which preserves the volume in the discretized level. Under a relatively mild and simple condition on $\gamma(\mathbf{n})$, we show that SP-PFEM is unconditionally energy-stable for almost all anisotropic surface energies $\gamma(\mathbf{n})$ arising in practical applications. Extensive numerical results are reported to demonstrate the efficiency and accuracy as well as energy dissipation of the proposed SP-PFEM for solving anisotropic surface diffusion in 3D.

Key words. Anisotropic surface diffusion, Cahn-Hoffman ξ -vector, anisotropic surface energy, parametric finite element method, structure-preserving, energy-stable, surface energy matrix

AMS subject classifications. 65M60, 65M12, 35K55, 53C44

1. Introduction. In materials science and solid-state physics as well as many other applications, surface energy is usually anisotropic due to lattice orientational anisotropy at material interfaces and/or surfaces [38, 24]. The anisotropic surface energy generates **anisotropic surface diffusion** – an important and general process involving the motion of adatoms, molecules and atomic clusters (adparticles) – at materials surfaces and interfaces in solids [18]. The anisotropic surface diffusion is an important kinetics and/or mechanism in surface phase formation [19], epitaxial growth [23, 25], heterogeneous catalysis [26], and other areas in materials/surface science [39]. It has significant and manifested applications in solid-state physics and materials science as well as computational geometry, such as solid-state dewetting [29, 35, 40, 39, 44], crystal growth of nanomaterials [15], evolution of voids in microelectronic circuits [33, 42], morphology development of alloys [2], quantum dots manufacturing [1], deformation of images [20], etc.

As is shown in Figure 1.1, for a closed surface $S := S(t)$ in three dimensions (3D) associated with a given anisotropic surface energy $\gamma(\mathbf{n})$, where $t \geq 0$ is time and $\mathbf{n} = (n_1, n_2, n_3)^T \in \mathbb{S}^2$ represents the outward unit normal vector satisfying $|\mathbf{n}| := \sqrt{n_1^2 + n_2^2 + n_3^2} = 1$, the motion by anisotropic surface diffusion of the surface is described by the following geometric flow [34, 29, 35, 40, 39, 44]:

$$(1.1) \quad V_n = \Delta_S \mu,$$

where V_n denotes the normal velocity, $\Delta_S := \nabla_S \cdot \nabla_S$ is the surface Laplace-Beltrami operator, ∇_S denotes the surface gradient with respect to the surface $S(t)$, and $\mu := \mu(\mathbf{n})$ is the chemical potential (or weighted mean curvature denoted as $H_\gamma := H_\gamma(\mathbf{n})$)

*Department of Mathematics, National University of Singapore, Singapore, 119076 (matbaowz@nus.edu.sg). This author's research was supported by the Ministry of Education of Singapore grant MOE2019-T2-1-063 (R-146-000-296-112).

†Department of Mathematics, National University of Singapore, Singapore, 119076 (e0444158@u.nus.edu).

in the literature) generated from the surface energy functional $W(S) := W(S(t)) = \int_{S(t)} \gamma(\mathbf{n}) dA$ with dA representing the surface integral via the thermodynamic variation as $\mu = \frac{\delta W(S)}{\delta S} = \lim_{\varepsilon \rightarrow 0} \frac{W(S^\varepsilon) - W(S)}{\varepsilon}$ with S^ε being a small perturbation of S [30, 31]. It is well-known that the evolution of the surface $S(t)$ under the anisotropic surface diffusion (1.1) preserves the following two essential geometric structures [18]: (1) the volume of the region enclosed by the surface is conserved, and (2) the free surface energy (or weighted surface area) $W(S)$ decreases in time. In fact, the motion governed by the anisotropic surface diffusion can be mathematically regarded as the H^{-1} -gradient flow of the free surface energy functional (or weighted surface area) $W(S)$ [37].

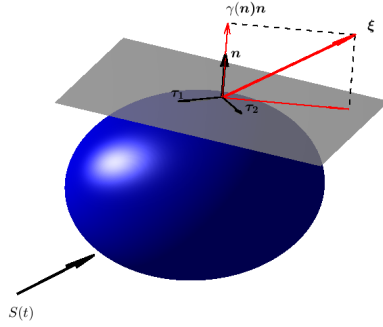


FIG. 1.1. An illustration of a closed surface $S(t)$ in \mathbb{R}^3 under anisotropic surface diffusion with an anisotropic surface energy $\gamma(\mathbf{n})$, where \mathbf{n} is the outward unit normal vector, ξ is the Cahn-Hoffman ξ -vector in (1.3), and τ_1 and τ_2 form a basis of the local tangential space.

Define $\gamma(\mathbf{p}) : \mathbb{R}_*^3 := \mathbb{R}^3 \setminus \{\mathbf{0}\} \rightarrow \mathbb{R}^+$ be a homogeneous extension of the anisotropic surface energy $\gamma(\mathbf{n}) : \mathbb{S}^2 \rightarrow \mathbb{R}^+$ satisfying: (i) $\gamma(c\mathbf{p}) = c\gamma(\mathbf{p})$ for $c > 0$ and $\mathbf{p} \in \mathbb{R}_*^3$, and (ii) $\gamma(\mathbf{p})|_{\mathbf{p}=\mathbf{n}} = \gamma(\mathbf{n})$ for $\mathbf{n} \in \mathbb{S}^2$. A typical homogeneous extension is widely used in the literature as [31, 21]

$$(1.2) \quad \gamma(\mathbf{p}) := |\mathbf{p}| \gamma\left(\frac{\mathbf{p}}{|\mathbf{p}|}\right), \quad \forall \mathbf{p} = (p_1, p_2, p_3)^T \in \mathbb{R}_*^3 := \mathbb{R}^3 \setminus \{\mathbf{0}\},$$

where $|\mathbf{p}| = \sqrt{p_1^2 + p_2^2 + p_3^2}$. Then the Cahn-Hoffman ξ -vector introduced by Cahn and Hoffman and the Hessian matrix $\mathbf{H}_\gamma(\mathbf{n})$ of $\gamma(\mathbf{p})$ are mathematically given by [28, 41]

$$(1.3) \quad \xi = (\xi_1, \xi_2, \xi_3)^T := \xi(\mathbf{n}) = \nabla \gamma(\mathbf{p})|_{\mathbf{p}=\mathbf{n}}, \quad \mathbf{H}_\gamma(\mathbf{n}) := \nabla \nabla \gamma(\mathbf{p})|_{\mathbf{p}=\mathbf{n}}, \quad \forall \mathbf{n} \in \mathbb{S}^2.$$

It is easy to check that $\xi \cdot \mathbf{n} = \gamma(\mathbf{n})$ for $\mathbf{n} \in \mathbb{S}^2$ [28, 41]. Then the chemical potential μ (or weighted mean curvature) can be obtained as [28]

$$(1.4) \quad \mu = \mu(\mathbf{n}) = H_\gamma = H_\gamma(\mathbf{n}) = \nabla_S \cdot \xi = \nabla_S \cdot \xi(\mathbf{n}), \quad \forall \mathbf{n} \in \mathbb{S}^2.$$

For any $\mathbf{n} \in \mathbb{S}^2$, we notice that $\mathbf{H}_\gamma(\mathbf{n})\mathbf{n} = \mathbf{0}$ and thus 0 is an eigenvalue of $\mathbf{H}_\gamma(\mathbf{n})$ and \mathbf{n} is a corresponding eigenvector. We denote the other two eigenvalues of $\mathbf{H}_\gamma(\mathbf{n})$

as $\lambda_1(\mathbf{n}) \leq \lambda_2(\mathbf{n}) \in \mathbb{R}$. When $\gamma(\mathbf{n}) \equiv \text{constant}$ (e.g. $\gamma(\mathbf{n}) \equiv 1$) for $\mathbf{n} \in \mathbb{S}^2$, i.e. with isotropic surface energy, then we have $\gamma(\mathbf{p}) = |\mathbf{p}|$ in (1.2), $\boldsymbol{\xi} = \mathbf{n}$ in (1.3), and $\mu = H$ and $\mathbf{H}_\gamma(\mathbf{n}) \equiv I_3 - \mathbf{n}\mathbf{n}^T$ in (1.3) with H the mean curvature and I_3 the 3×3 identity matrix and $\lambda_1(\mathbf{n}) = \lambda_2(\mathbf{n}) \equiv 1$, and thus the anisotropic surface diffusion (1.1) collapses to the (isotropic) surface diffusion with normal velocity given as $V_n = \Delta_S H$ [10, 34]. In contrast, when $\gamma(\mathbf{n})$ is not a constant, i.e. with anisotropic surface energy: when $\boldsymbol{\tau}^T \mathbf{H}_\gamma(\mathbf{n}) \boldsymbol{\tau} \geq 0$ for all $\mathbf{n}, \boldsymbol{\tau} \in \mathbb{S}^2$ satisfying $\boldsymbol{\tau} \cdot \mathbf{n} := \boldsymbol{\tau}^T \mathbf{n} = 0$ ($\Leftrightarrow \lambda_2(\mathbf{n}) \geq \lambda_1(\mathbf{n}) \geq 0$ for all $\mathbf{n} \in \mathbb{S}^2 \Leftrightarrow$ the Frank diagram of $\gamma(\mathbf{n})$ is convex), it is called as *weakly anisotropic*; and when $\boldsymbol{\tau}^T \mathbf{H}_\gamma(\mathbf{n}) \boldsymbol{\tau}$ changes sign for $\mathbf{n}, \boldsymbol{\tau} \in \mathbb{S}^2$ satisfying $\boldsymbol{\tau} \cdot \mathbf{n} = 0$ ($\Leftrightarrow \lambda_1(\mathbf{n}) < 0$ for some $\mathbf{n} \in \mathbb{S}^2 \Leftrightarrow$ the Frank diagram of $\gamma(\mathbf{n})$ is not convex), it is called as *strongly anisotropic*. For convenience of readers, we list several commonly-used anisotropic surface energies $\gamma(\mathbf{n})$ in the literature and their corresponding Cahn-Hoffman $\boldsymbol{\xi}$ -vectors in Appendix A.

Different numerical methods have been presented for solving the isotropic/anisotropic surface diffusion (1.1), such as the finite element method via graph evolution [3, 21], the marker-particle method [22], the discontinuous Galerkin finite element method [43], and the parametric finite element method (PFEM) [10, 13, 27, 7, 31, 32]. Among these methods, for isotropic surface diffusion, the energy-stable PFEM (ES-PFEM) based on an elegant variational formulation, which was proposed by Barrett, Garcke, and Nürnberg [10, 12] (denoted as BGN scheme), performs the best in terms of efficiency and accuracy as well as mesh quality in practical computations, especially in two dimensions (2D). The BGN scheme with unconditionally energy stability was successfully extended for solving solid-state dewetting problems with isotropic surface energy, i.e. motion of open curve and surface in 2D and 3D, respectively [10, 12]. It was also successfully extended for solving anisotropic surface diffusion with the Riemannian metric anisotropic surface energy [11, 13]. Recently, based on BGN's variational formulation for surface diffusion, by approximating the normal vector in a clever way, Bao and Zhao [9, 5, 4] presented a structure-preserving PFEM (SP-PFEM) for surface diffusion, which preserves area/volume conservation in 2D/3D and unconditionally energy dissipation in the discretized level. Very recently, by introducing a proper surface energy matrix depending on the Cahn-Hoffman $\boldsymbol{\xi}$ -vector and a stabilizing function in 2D, we obtained a new symmetrized (and conservative) variational formulation for anisotropic surface diffusion with arbitrary surface energy in 2D and then designed structure-preserving and energy-stable PFEM under mild and simple conditions on the surface energy [6]. The main aim of this paper is to extend the above method from 2D to 3D for anisotropic surface diffusion with arbitrary surface energy. Again, the key is based on introducing a proper surface energy matrix depending on the Cahn-Hoffman $\boldsymbol{\xi}$ -vector and a stabilizing function in 3D and obtaining a new symmetrized (and conservative) variational formulation. The difficulty and major part is to establish unconditionally energy dissipation of the full discretization under the following simple and mild condition on the arbitrary surface energy $\gamma(\mathbf{n})$ as

$$(1.5) \quad \gamma(-\mathbf{n}) = \gamma(\mathbf{n}), \quad \forall \mathbf{n} \in \mathbb{S}^2, \quad \gamma(\mathbf{p}) \in C^2(\mathbb{R}^3 \setminus \{\mathbf{0}\}).$$

The paper is organized as follows. In section 2, we recall the mathematical representations for anisotropic surface diffusion, obtain a symmetrized variational formulation and propose a SP-PFEM to discretize it. In section 3, we establish energy stability of the proposed SP-PFEM. Extensive numerical results are reported to demonstrate the efficiency and accuracy as well as structure-preserving properties in section 4. Finally, some conclusions are drawn in section 5.

2. A new symmetrized variational formulation and its discretization.

We begin with a mathematical representation for the anisotropic surface diffusion in 3D, introduce a symmetric positive surface energy matrix $\mathbf{Z}_k(\mathbf{n})$, and obtain a symmetrized conservative variational formulation for anisotropic surface diffusion in 3D. A SP-PFEM is presented to discretize the variational formulation and some structural preserving properties are established.

2.1. A mathematical representation for anisotropic surface diffusion.

Let the closed surface $S := S(t)$ be parameterized by $\mathbf{X}(\cdot, t)$ as

$$(2.1) \quad \mathbf{X}(\cdot, t) : U \rightarrow \mathbb{R}^3, \quad \rho \mapsto \mathbf{X}(\rho, t) = (X_1(\rho, t), X_2(\rho, t), X_3(\rho, t))^T, \quad \rho \in U,$$

where $U \subset \mathbb{R}^2$ is a bounded domain, then the motion of $S(t)$ under the anisotropic surface diffusion (1.1) can be mathematically described by the following geometric partial differential equations (PDEs) via the Cahn-Hoffman ξ -vector as [21]

$$(2.2a) \quad \partial_t \mathbf{X}(\rho, t) = (\Delta_S \mu) \mathbf{n}, \quad \rho \in U, \quad t > 0,$$

$$(2.2b) \quad \left\{ \begin{array}{l} \mu = \nabla_S \cdot \xi, \\ \xi = \nabla \gamma(\mathbf{p}) \big|_{\mathbf{p}=\mathbf{n}}. \end{array} \right.$$

The anisotropic surface diffusion (2.2) can also be regarded as a geometric flow from the given initial closed surface $S_0 := S(0) \subset \mathbb{R}^3$, which is parameterized by $\mathbf{X}_0 := \mathbf{X}(\cdot, 0)$, to the surface $S(t) \subset \mathbb{R}^3$. Via the parametrization $\mathbf{X}(\cdot, t)$ of $S(t)$, we remark here that any function $u : S(t) \rightarrow \mathbb{R}$ can be regarded as a function $\tilde{u} : U \rightarrow \mathbb{R}$ as: $\tilde{u}(\rho) := u(\mathbf{X}(\rho, t))$ for $\rho \in U$; and vice versa, any function $\tilde{u} : U \rightarrow \mathbb{R}$ can be regarded as a function $u : S(t) \rightarrow \mathbb{R}$ as: $u(\mathbf{X}) := \tilde{u}(\rho^{-1}(\mathbf{X}))$ for $\mathbf{X} \in S(t)$, where $\rho^{-1}(\cdot)$ is the (locally) inverse mapping from $S(t)$ to U . With this understanding, we define the function spaces over the evolving surface $S(t)$ as

$$(2.3) \quad L^2(S(t)) := \left\{ u : S(t) \rightarrow \mathbb{R} \mid \int_{S(t)} |u|^2 dA < \infty \right\},$$

equipped with the L^2 -inner product

$$(2.4) \quad (u, v)_{S(t)} := \int_{S(t)} u v dA, \quad \forall u, v \in L^2(S(t)).$$

We remark here that $L^2(S(t))$ is equivalent to $L^2(S_0)$ and also is equivalent to $L^2(\Omega)$. The above inner product can be extended to $[L^2(S(t))]^3$ by replacing the scalar product uv by the vector inner product $\mathbf{u} \cdot \mathbf{v}$. And we adopt the angle bracket to emphasize the inner product for two matrix-valued functions \mathbf{U}, \mathbf{V} in $[L^2(S(t))]^{3 \times 3}$ as

$$(2.5) \quad \langle \mathbf{U}, \mathbf{V} \rangle_{S(t)} := \int_{S(t)} \mathbf{U} : \mathbf{V} dA, \quad \forall \mathbf{U}, \mathbf{V} \in [L^2(S(t))]^{3 \times 3},$$

here $\mathbf{U} : \mathbf{V} = \text{Tr}(\mathbf{V}^T \mathbf{U})$ is the Frobenius inner product with $\text{Tr}(\mathbf{U})$ denoting the trace of a matrix $\mathbf{U} \in \mathbb{R}^{3 \times 3}$. Furthermore, we introduce the Sobolev space

$$(2.6) \quad H^1(S(t)) := \left\{ u : S(t) \rightarrow \mathbb{R} \mid u \in L^2(S(t)), \nabla_S u \in [L^2(S(t))]^3 \right\}.$$

And this definition can be extended easily to $[H^1(S(t))]^3$. We adopt the notation $\nabla_S f = (\underline{D}_1 f, \underline{D}_2 f, \underline{D}_3 f)^T$ for a scalar-valued function f [21], and the surface gradient for a vector-valued function $\mathbf{F} = (F_1, F_2, F_3)^T$ is defined as

$$(2.7) \quad \nabla_S \mathbf{F} := (\nabla_S F_1, \nabla_S F_2, \nabla_S F_3)^T \in \mathbb{R}^{3 \times 3}.$$

2.2. A new symmetrized variational formulation and its property. Introducing the symmetric surface energy matrix $\mathbf{Z}_k(\mathbf{n})$

$$(2.8) \quad \begin{aligned} \mathbf{Z}_k(\mathbf{n}) &= \gamma(\mathbf{n})I_3 - \mathbf{n}\boldsymbol{\xi}^T(\mathbf{n}) - \boldsymbol{\xi}(\mathbf{n})\mathbf{n}^T + k(\mathbf{n})\mathbf{n}\mathbf{n}^T \\ &= \gamma(\mathbf{n})I_3 - \mathbf{n}\boldsymbol{\xi}^T - \boldsymbol{\xi}\mathbf{n}^T + k(\mathbf{n})\mathbf{n}\mathbf{n}^T, \quad \forall \mathbf{n} \in \mathbb{S}^2, \end{aligned}$$

where $k(\mathbf{n}) : \mathbb{S}^2 \rightarrow \mathbb{R}^+$ is a stabilizing function which ensures $\mathbf{Z}_k(\mathbf{n})$ is positive definite, it is easy to see that the above matrix is a direct generalization from 2D to 3D as proposed in [6]. Then we obtain a symmetric and conservative variational (weak) formulation for the chemical potential (or weighted mean curvature) μ via the matrix $\mathbf{Z}_k(\mathbf{n})$. We remark here that, in 2D case, we can obtain both strong (PDE) and weak (variational) formulation for the chemical potential (or weighted curvature) μ ; however, in 3D case, it is not easy to write a simple strong (PDE) formulation for the chemical potential (or weighted mean curvature) μ via the matrix $\mathbf{Z}_k(\mathbf{n})$.

LEMMA 2.1 (weak formulation for μ). *The weighted mean curvature μ satisfies the following weak formulation.*

$$(2.9) \quad (\mu, \mathbf{n} \cdot \boldsymbol{\omega})_S = \langle \mathbf{Z}_k(\mathbf{n})\nabla_S \mathbf{X}, \nabla_S \boldsymbol{\omega} \rangle_S, \quad \forall \boldsymbol{\omega} = (\omega_1, \omega_2, \omega_3)^T \in [H^1(S(t))]^3.$$

Proof. Noticing the fact $\underline{D}_i X_k = \delta_{i,k} - n_k n_i$ and $\nabla_S f \cdot \mathbf{n} = 0$ [21], we obtain

$$(2.10) \quad \nabla_S X_k \cdot \nabla_S \omega_l = \sum_{i=1}^3 (\delta_{i,k} - n_k n_i) \underline{D}_i \omega_l = \underline{D}_k \omega_l - n_k \nabla_S \omega_l \cdot \mathbf{n} = \underline{D}_k \omega_l.$$

Substituting the identity (2.10) into [21, equation (8.18)] yields the following identity

$$(2.11) \quad (\mu, \mathbf{n} \cdot \boldsymbol{\omega})_S = \gamma(\mathbf{n}) \sum_{l=1}^3 \int_{S(t)} \nabla_S X_l \cdot \nabla_S \omega_l \, dS - \sum_{k,l=1}^3 \int_{S(t)} \xi_k n_l \nabla_S X_k \cdot \nabla_S \omega_l \, dS.$$

Obviously, the second term $\langle \gamma(\mathbf{n})\nabla_S \mathbf{X}, \nabla_S \boldsymbol{\omega} \rangle_S$ corresponds to $\gamma(\mathbf{n})I_3$ in $\mathbf{Z}_k(\mathbf{n})$. Now by simplifying the last term, we have

$$(2.12) \quad \begin{aligned} \sum_{k,l=1}^3 \int_S \xi_k n_l \nabla_S X_k \cdot \nabla_S \omega_l \, dA &= \int_S \left(\sum_{k=1}^3 \xi_k (\nabla_S X_k) \right) \cdot \left(\sum_{l=1}^3 n_l (\nabla_S \omega_l) \right) \, dA \\ &= \int_S ((\nabla_S \mathbf{X})^T \boldsymbol{\xi}) \cdot ((\nabla_S \boldsymbol{\omega})^T \mathbf{n}) \, dA \\ &= \int_S \text{Tr} \left((\nabla_S \boldsymbol{\omega})^T \mathbf{n} \boldsymbol{\xi}^T (\nabla_S \mathbf{X}) \right) \, dA \\ &= \int_S (\mathbf{n} \boldsymbol{\xi}^T (\nabla_S \mathbf{X})) : (\nabla_S \boldsymbol{\omega}) \, dA \\ &= \langle \mathbf{n} \boldsymbol{\xi}^T \nabla_S \mathbf{X}, \nabla_S \boldsymbol{\omega} \rangle_S, \end{aligned}$$

which is the $\mathbf{n}\boldsymbol{\xi}^T(\mathbf{n})$ part in $\mathbf{Z}_k(\mathbf{n})$.

Finally, recalling the identity $\nabla_S \mathbf{X} = I_3 - \mathbf{n}\mathbf{n}^T$ and combining the two identities (2.11) and (2.12) yields

$$(2.13) \quad \begin{aligned} (\mu, \mathbf{n} \cdot \boldsymbol{\omega})_S &= \langle (\gamma(\mathbf{n})I_3 - \mathbf{n}\boldsymbol{\xi}^T) \nabla_S \mathbf{X}, \nabla_S \boldsymbol{\omega} \rangle_S \\ &= \langle \mathbf{Z}_k(\mathbf{n}) \nabla_S \mathbf{X}, \nabla_S \boldsymbol{\omega} \rangle_S + \langle (\boldsymbol{\xi}\mathbf{n}^T - k(\mathbf{n})\mathbf{n}\mathbf{n}^T)(I_3 - \mathbf{n}\mathbf{n}^T), \nabla_S \boldsymbol{\omega} \rangle_S \\ &= \langle \mathbf{Z}_k(\mathbf{n}) \nabla_S \mathbf{X}, \nabla_S \boldsymbol{\omega} \rangle_S, \end{aligned}$$

which is the desired result. \square

With the weak formulation of μ (2.9) given in lemma 2.1, by taking integration by parts, we can easily derive the following variational formulation for the anisotropic surface diffusion (2.2) (or (1.1)): For a given closed initial surface $S_0 := S(0)$, find the solution $(\mathbf{X}(\cdot, t), \mu(\cdot, t)) \in [H^1(S(t))]^3 \times H^1(S(t))$ such that

$$(2.14a) \quad (\partial_t \mathbf{X} \cdot \mathbf{n}, \psi)_{S(t)} + (\nabla_S \mu, \nabla_S \psi)_{S(t)} = 0 \quad \forall \psi \in H^1(S(t)),$$

$$(2.14b) \quad (\mu \mathbf{n}, \boldsymbol{\omega})_{S(t)} - \langle Z_k(\mathbf{n}) \nabla_S \mathbf{X}, \nabla_S \boldsymbol{\omega} \rangle_{S(t)} = 0 \quad \forall \boldsymbol{\omega} \in [H^1(S(t))]^3.$$

Denote the enclosed volume and the free energy of $S(t)$ as $V(t)$ and $W(t)$, respectively, which are defined by

$$(2.15) \quad V(t) := \frac{1}{3} \int_{S(t)} \mathbf{X} \cdot \mathbf{n} \, dA, \quad W(t) := \int_{S(t)} \gamma(\mathbf{n}) \, dA.$$

For the weak formulation (2.14), by applying the Reynolds transport theorem [17, Theorem 32, Theorem 33] and Lemma 97 in [17], similar to the proof of proposition 2.2 in [8], we know that the the volume $V(t)$ is conserved and the energy $W(t)$ is dissipative.

PROPOSITION 2.1 (volume conservation and energy dissipation). *The variational problem (2.14) preserves volume conservation and energy dissipation as*

$$(2.16a) \quad V(t) \equiv V(0) := \frac{1}{3} \int_{S_0} \mathbf{X}_0 \cdot \mathbf{n} \, dA, \quad t \geq 0,$$

$$(2.16b) \quad W(t) \leq W(t') \leq W(0) := \int_{S_0} \gamma(\mathbf{n}) \, dA, \quad t \geq t' \geq 0.$$

2.3. A structural-preserving parametric finite element method (SP-PFEM). We take $\tau > 0$ to be the time step size, and the discrete time levels are $t_m = m\tau$ for each $m \geq 0$. For spatial discretization, as illustrated in figure 2.1, the surface $S(t_m)$ is approximated by a polyhedron $S^m = \cup_{j=1}^J \overline{\sigma_j^m}$ with J mutually disjoint non-degenerated triangular surfaces σ_j^m and I vertices \mathbf{q}_i^m . We further denote $\{\mathbf{q}_{j_1}^m, \mathbf{q}_{j_2}^m, \mathbf{q}_{j_3}^m\}$ as the three counterclockwise vertices of the triangle σ_j^m , and $\mathcal{J}\{\sigma_j^m\} := (\mathbf{q}_{j_2}^m - \mathbf{q}_{j_1}^m) \times (\mathbf{q}_{j_3}^m - \mathbf{q}_{j_1}^m)$ is the orientation vector with respect to σ_j^m , and the outward unit normal vector \mathbf{n}_j^m of σ_j^m is thus given by $\mathbf{n}_j^m = \frac{\mathcal{J}\{\sigma_j^m\}}{|\mathcal{J}\{\sigma_j^m\}|}$ for $1 \leq j \leq J$.

The finite element space with respect to the surface $S^m = \cup_{j=1}^J \overline{\sigma_j^m}$ is defined as

$$(2.17) \quad \mathbb{K}^m := \left\{ u \in C(S^m) \mid u|_{\sigma_j^m} \in \mathcal{P}^1(\sigma_j^m), \forall 1 \leq j \leq J \right\},$$

which is equipped with the mass lumped inner product $(\cdot, \cdot)_{S^m}^h$ with h denoting the mesh size of S^m as

$$(2.18) \quad (f, g)_{S^m}^h := \frac{1}{3} \sum_{j=1}^J \sum_{i=1}^3 |\sigma_j^m| f((\mathbf{q}_{j_i}^m)^-) g((\mathbf{q}_{j_i}^m)^-),$$

where $\mathcal{P}^1(\sigma_j^m)$ is the space of polynomials on σ_j^m with degree at almost 1, $|\sigma_j^m| := \frac{1}{2} |\mathcal{J}\{\sigma_j^m\}|$ denotes the area of σ_j^m , and $f((\mathbf{q}_{j_i}^m)^-)$ means the one-sided limit of $f(\mathbf{x})$

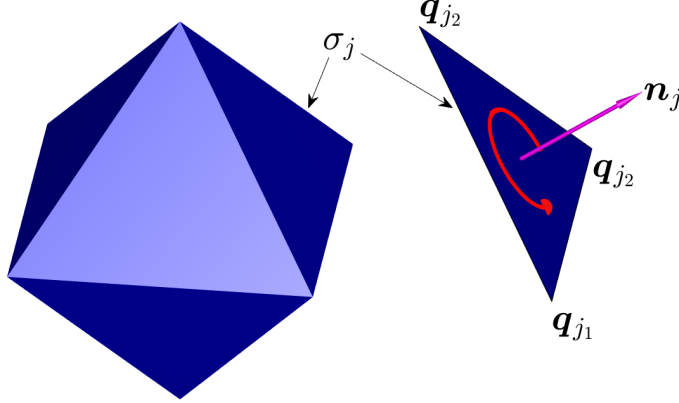


FIG. 2.1. An illustration of the approximation polyhedron S^0 : the vertices $\{q_{j_1}, q_{j_2}, q_{j_3}\}$ of the triangle σ_j is oriented counterclockwise, see the red circular arrow; and the direction of the normal vector n_j is determined by the right-hand rule.

at $q_{j_i}^m$ inside σ_j^m . This definition is also valid for vector- and matrix-valued function, and the mass lumped inner product of the matrix-valued functions \mathbf{U} and \mathbf{V} is also emphasized by the angle bracket as

$$(2.19) \quad \langle \mathbf{U}, \mathbf{V} \rangle_{S^m}^h := \frac{1}{3} \sum_{j=1}^J \sum_{i=1}^3 |\sigma_j^m| \mathbf{U}((q_{j_i}^m)^-) : \mathbf{V}((q_{j_i}^m)^-).$$

We remark here that $(f, g)_{S^m}^h$ and $\langle \mathbf{U}, \mathbf{V} \rangle_{S^m}^h$ can be viewed as approximations of $(f, g)_{S^m}$ and $\langle \mathbf{U}, \mathbf{V} \rangle_{S^m}$, respectively. Finally, the discretized surface gradient operator ∇_S for $f \in \mathbb{K}^m$ is given by

$$(2.20) \quad \nabla_S f|_{\sigma_j^m} := \left(f(q_{j_1}^m)(q_{j_2}^m - q_{j_3}^m) + f(q_{j_2}^m)(q_{j_3}^m - q_{j_1}^m) + f(q_{j_3}^m)(q_{j_1}^m - q_{j_2}^m) \right) \times \frac{\mathbf{n}_j^m}{|\mathcal{J}\{\sigma_j^m\}|},$$

and for vector-valued function $\mathbf{F} = (F_1, F_2, F_3)^T \in [\mathbb{K}^m]^3$, $\nabla_S \mathbf{F} := (\nabla_S F_1, \nabla_S F_2, \nabla_S F_3)^T$.

A fully-implicit structural-preserving finite element method (SP-PFEM) for the variational formulation (2.14) can then be stated as follows: Given the initial approximation $S^0 = \cup_{j=1}^J \sigma_j^0$ of $S(0)$; for each time step $t_m = m\tau$ ($m \geq 0$), find the solution $(\mathbf{X}^{m+1}, \mu^{m+1}) \in [\mathbb{K}^m]^3 \times \mathbb{K}^m$ such that

$$(2.21a) \quad \left(\frac{\mathbf{X}^{m+1} - \mathbf{X}^m}{\tau} \cdot \mathbf{n}^{m+\frac{1}{2}}, \psi \right)_{S^m}^h + (\nabla_S \mu^{m+1}, \nabla_S \psi)_{S^m}^h = 0, \quad \forall \psi \in \mathbb{K}^m,$$

$$(2.21b) \quad \left(\mu^{m+1} \mathbf{n}^{m+\frac{1}{2}}, \boldsymbol{\omega} \right)_{S^m}^h - \langle \mathbf{Z}_k(\mathbf{n}^m) \nabla_S \mathbf{X}^{m+1}, \nabla_S \boldsymbol{\omega} \rangle_{S^m}^h = 0, \quad \forall \boldsymbol{\omega} \in [\mathbb{K}^m]^3.$$

Here $\mathbf{X}^m(\mathbf{q}_i^m) = \mathbf{q}_i^m$, $\mathbf{X}^{m+1}(\mathbf{q}_i^m) = \mathbf{q}_i^{m+1}$ for each i , $\mathbf{n}^m|_{\sigma_j^m} = \mathbf{n}_j^m$, $\sigma_j^{m+1} = \mathbf{X}^{m+1}(\sigma_j^m)$ is the triangle with counterclockwisely ordered vertices $\{\mathbf{q}_{j_1}^{m+1}, \mathbf{q}_{j_2}^{m+1}, \mathbf{q}_{j_3}^{m+1}\}$ for each j , and $S^{m+1} = \cup_{j=1}^J \overline{\sigma_j^{m+1}}$ for each m . The semi-implicit approximation $\mathbf{n}^{m+\frac{1}{2}}$ of the outward normal vector \mathbf{n} at $t = (m + \frac{1}{2})\tau$ is defined as follows

$$(2.22) \quad \mathbf{n}^{m+\frac{1}{2}}|_{\sigma_j^m} := \frac{\mathcal{J}\{\sigma_j^m\} + 4\mathcal{J}\{\sigma_j^{m+\frac{1}{2}}\} + \mathcal{J}\{\sigma_j^{m+1}\}}{6|\mathcal{J}\{\sigma_j^m\}|},$$

where $\sigma_j^{m+\frac{1}{2}} := \frac{1}{2}(\sigma_j^m + \sigma_j^{m+1})$.

REMARK 2.1. *We note the function \mathbf{X}^{m+1} has different meanings at time step t_m (as a function in $[\mathbb{K}^m]^3$) and t_{m+1} (as a function in $[\mathbb{K}^{m+1}]^3$), and we adopt the same notation for simplicity.*

2.4. Main results. For the discretized polygon surface $S^m = \cup_{j=1}^J \overline{\sigma_j^m}$, its enclosed volume and surface energy are denoted as V^m and W^m , respectively, which are defined as

$$(2.23a) \quad V^m := \frac{1}{3} \int_{S^m} \mathbf{X}^m \cdot \mathbf{n}^m dA = \frac{1}{9} \sum_{j=1}^J \sum_{i=1}^3 |\sigma_j^m| \mathbf{q}_{j_i}^m \cdot \mathbf{n}_j^m,$$

$$(2.23b) \quad W^m := \int_{S^m} \gamma(\mathbf{n}^m) dA = \sum_{j=1}^J |\sigma_j^m| \gamma(\mathbf{n}_j^m), \quad \forall m \geq 0.$$

For the SP-PFEM (2.21), we have

THEOREM 2.2 (structural-preserving). *For any given surface energy $\gamma(\mathbf{n})$ satisfying the energy stable condition (1.5), there exists a minimal stabilizing function $k_0(\mathbf{n}) : \mathbb{S}^2 \rightarrow \mathbb{R}^+$, such that when the stabilizing function $k(\mathbf{n})$ is taken as $k(\mathbf{n}) \geq k_0(\mathbf{n})$ for $\mathbf{n} \in \mathbb{S}^2$ in the surface energy matrix $Z_k(\mathbf{n})$ in (2.8), then the SP-PFEM (2.21) is volume conservative and unconditionally energy stable, i.e.*

$$(2.24a) \quad V^{m+1} = V^m = \dots = V^0, \quad \forall m \geq 0,$$

$$(2.24b) \quad W^{m+1} \leq W^m \leq \dots \leq W^0, \quad \forall m \geq 0.$$

The proof of volume conservation (2.24a) is similar to [9], and we omit it here for brevity; and the unconditional energy stability (2.24b) will be established in the next section.

REMARK 2.2. *The SP-PFEM (2.21) is implicit, i.e. at each time step, one needs to solve a nonlinear coupled system, which can be solved efficiently by the Newton's method. Of course, if we simply replace $\mathbf{n}^{m+\frac{1}{2}}$ in (2.21) by \mathbf{n}^m , we can obtain a semi-implicit energy-stable PFEM (ES-PFEM), where only a linear system needs to be solved at each time. Of course for the semi-implicit ES-PFEM, the volume conservation is no longer valid. Under the same condition as in Theorem 2.2, the ES-PFEM is also unconditionally energy stable.*

REMARK 2.3. *The semi-discretization in space by the PFEM of the variational problem (2.14) also preserves the two geometric properties. And the proof is similar to the isotropic case; we refer [10, 45, 9] for the result of semi-discretization of 3D isotropic surface diffusion.*

3. Energy stability. In this section, by showing the existence of the minimal stabilizing function $k_0(\mathbf{n}) : \mathbb{S}^2 \rightarrow \mathbb{R}^+$, we prove the unconditional energy stability of the SP-PFEM (2.21) when the surface energy $\gamma(\mathbf{n})$ satisfies (1.5).

3.1. The minimal stabilizing function. We define an axillary function $F_k(\mathbf{n}, \mathbf{u}, \mathbf{v}) : [\mathbb{S}^2]^3 \rightarrow \mathbb{R}$ as

$$(3.1) \quad F_k(\mathbf{n}, \mathbf{u}, \mathbf{v}) := (\mathbf{u}^T \mathbf{Z}_k(\mathbf{n}) \mathbf{u}) (\mathbf{v}^T \mathbf{Z}_k(\mathbf{n}) \mathbf{v}), \quad \mathbf{n}, \mathbf{u}, \mathbf{v} \in \mathbb{S}^2,$$

then the minimal stabilizing function $k_0(\mathbf{n}) : \mathbb{S}^2 \rightarrow \mathbb{R}^+$ is given by

$$(3.2) \quad k_0(\mathbf{n}) = \inf \left\{ k(\mathbf{n}) \mid F_k(\mathbf{n}, \mathbf{u}, \mathbf{v}) \geq \gamma^2(\mathbf{u} \times \mathbf{v}), \quad \forall \mathbf{u}, \mathbf{v} \in \mathbb{S}^2 \right\}, \quad \mathbf{n} \in \mathbb{S}^2.$$

From (3.2), we know that $F_{k_0}(\mathbf{n}, \mathbf{u}, \mathbf{v}) \geq 0$ for $\mathbf{n}, \mathbf{u}, \mathbf{v} \in \mathbb{S}^2$. Taking $k = k_0$, $\mathbf{u} = \mathbf{n}$ and $\mathbf{v} = \boldsymbol{\tau} \in \mathbb{S}^2$ satisfying $\boldsymbol{\tau} \cdot \mathbf{n} = 0$ in (3.1), noticing $\boldsymbol{\tau}^T \mathbf{Z}_{k_0}(\mathbf{n}) \boldsymbol{\tau} = \gamma(\mathbf{n}) > 0$ and $\mathbf{n} \cdot \boldsymbol{\xi} = \gamma(\mathbf{n})$, we obtain

$$(3.3) \quad 0 \leq \mathbf{n}^T \mathbf{Z}_{k_0}(\mathbf{n}) \mathbf{n} = k_0(\mathbf{n}) - \gamma(\mathbf{n}) \Rightarrow k_0(\mathbf{n}) \geq \gamma(\mathbf{n}) > 0, \quad \mathbf{n} \in \mathbb{S}^2.$$

To prove the existence of $k_0(\mathbf{n})$, for any given $\mathbf{n} \in \mathbb{S}^2$, we only need to show there exists a $k(\mathbf{n})$ sufficiently large such that $F_k(\mathbf{n}, \mathbf{u}, \mathbf{v}) \geq \gamma^2(\mathbf{u} \times \mathbf{v})$ for any $\mathbf{u}, \mathbf{v} \in \mathbb{S}^2$.

LEMMA 3.1. *Let $G(\mathbf{n}, \mathbf{u}, \mathbf{v})$ be another axillary function given by*

$$(3.4) \quad G(\mathbf{n}, \mathbf{u}, \mathbf{v}) := \gamma(\mathbf{n}) [\gamma(\mathbf{n}) - 2(\boldsymbol{\xi} \cdot \mathbf{u})(\mathbf{n} \cdot \mathbf{u}) - 2(\boldsymbol{\xi} \cdot \mathbf{v})(\mathbf{n} \cdot \mathbf{v})], \quad \mathbf{n}, \mathbf{u}, \mathbf{v} \in \mathbb{S}^2,$$

then for any $k(\mathbf{n}) > 0$, the following inequality holds

$$(3.5) \quad F_k(\mathbf{n}, \mathbf{u}, \mathbf{v}) - G(\mathbf{n}, \mathbf{u}, \mathbf{v}) \geq [\gamma(\mathbf{n})k(\mathbf{n}) - 4|\boldsymbol{\xi}|^2] [(n \cdot \mathbf{u})^2 + (n \cdot \mathbf{v})^2].$$

Proof. By direct computation and the arithmetic-geometric mean inequality, we obtain

$$\begin{aligned} & F_k(\mathbf{n}, \mathbf{u}, \mathbf{v}) - G(\mathbf{n}, \mathbf{u}, \mathbf{v}) \\ & \geq \gamma(\mathbf{n})k(\mathbf{n}) [(n \cdot \mathbf{u})^2 + (n \cdot \mathbf{v})^2] + k(\mathbf{n})^2 (n \cdot \mathbf{u})^2 (n \cdot \mathbf{v})^2 \\ & \quad - 4|\boldsymbol{\xi}|^2 |(n \cdot \mathbf{u})(n \cdot \mathbf{v})| - 2|\boldsymbol{\xi}| k(\mathbf{n}) |(n \cdot \mathbf{u})(n \cdot \mathbf{v})| (|n \cdot \mathbf{u}| + |n \cdot \mathbf{v}|) \\ & \geq [\gamma(\mathbf{n})k(\mathbf{n}) - 2|\boldsymbol{\xi}|^2] [(n \cdot \mathbf{u})^2 + (n \cdot \mathbf{v})^2] + k(\mathbf{n})^2 (n \cdot \mathbf{u})^2 (n \cdot \mathbf{v})^2 \\ & \quad - k(\mathbf{n}) |\boldsymbol{\xi}| \left[(n \cdot \mathbf{u})^2 \left(\frac{2|\boldsymbol{\xi}|}{k(\mathbf{n})} + \frac{k(\mathbf{n})}{2|\boldsymbol{\xi}|} (n \cdot \mathbf{v})^2 \right) + (n \cdot \mathbf{v})^2 \left(\frac{2|\boldsymbol{\xi}|}{k(\mathbf{n})} + \frac{k(\mathbf{n})}{2|\boldsymbol{\xi}|} (n \cdot \mathbf{u})^2 \right) \right] \\ & = [\gamma(\mathbf{n})k(\mathbf{n}) - 4|\boldsymbol{\xi}|^2] [(n \cdot \mathbf{u})^2 + (n \cdot \mathbf{v})^2], \end{aligned}$$

which is the desired inequality (3.5). \square

Since $\gamma(\mathbf{p})$ is not differentiable at $\mathbf{p} = \mathbf{0}$, the cross product $\gamma^2(\mathbf{u} \times \mathbf{v}) \notin C^2(\mathbb{S}^2 \times \mathbb{S}^2)$. The following lemma is helpful in estimating $\gamma^2(\mathbf{u} \times \mathbf{v})$.

LEMMA 3.2. *For any $\gamma(\mathbf{n})$ satisfying (1.5), then $\gamma^2(\mathbf{p})$ is continuous differentiable in \mathbb{R}^3 . Moreover, there exists a constant C_1 defined by*

$$(3.6) \quad C_1 = \frac{1}{2} \sup_{\mathbf{n} \in \mathbb{S}^2} \|\mathbf{H}_{\gamma^2}(\mathbf{n})\|_2,$$

where $\|\cdot\|_2$ is the spectral norm, such that

$$(3.7) \quad \gamma^2(\mathbf{p}) - \gamma^2(\mathbf{q}) \leq \nabla(\gamma^2(\mathbf{q})) \cdot (\mathbf{p} - \mathbf{q}) + C_1 |\mathbf{p} - \mathbf{q}|^2, \quad \forall \mathbf{p}, \mathbf{q} \in \mathbb{R}^3.$$

Proof. It is straightforward to check $\gamma^2(\mathbf{p}) \in C^1(\mathbb{R}^3)$ by definition.

To prove the inequality (3.7), we first consider the case that the line segment of \mathbf{p}, \mathbf{q} does not pass $\mathbf{0}$, i.e., $\lambda\mathbf{p} + (1 - \lambda)\mathbf{q} \neq \mathbf{0}$ for all $0 \leq \lambda \leq 1$. Since $\gamma^2(\mathbf{p})$ is homogeneous of degree 2, we know that $\mathbf{H}_{\gamma^2}(\mathbf{p})$ is homogeneous of degree 0, which yields

$$(3.8) \quad \mathbf{H}_{\gamma^2}(\zeta) = \mathbf{H}_{\gamma^2}(\zeta/|\zeta|), \quad \forall \mathbf{0} \neq \zeta \in \mathbb{R}^3.$$

By the mean value theorem, there exists a $\lambda_0 \in (0, 1)$ and $\zeta = \lambda_0\mathbf{p} + (1 - \lambda_0)\mathbf{q} \neq \mathbf{0}$, such that

$$(3.9) \quad \gamma^2(\mathbf{p}) = \gamma^2(\mathbf{q}) + \nabla(\gamma^2(\mathbf{q})) \cdot (\mathbf{p} - \mathbf{q}) + \frac{1}{2}(\mathbf{p} - \mathbf{q})^T \mathbf{H}_{\gamma^2}(\zeta)(\mathbf{p} - \mathbf{q}).$$

Thus (3.7) holds for such \mathbf{p}, \mathbf{q} .

If $\mathbf{0}$ is contained in line segment of \mathbf{p}, \mathbf{q} , we can find a sequence $(\mathbf{p}_k, \mathbf{q}_k) \rightarrow (\mathbf{p}, \mathbf{q})$ such that for each k , the line segment of $\mathbf{p}_k, \mathbf{q}_k$ does not pass $\mathbf{0}$. We know (3.7) holds for such $\mathbf{p}_k, \mathbf{q}_k$. By using the continuity of $\gamma^2(\mathbf{p})$ and $\nabla(\gamma^2(\mathbf{p}))$, we obtain that (3.7) is valid in this case by letting $k \rightarrow \infty$.

Thus the inequity (3.7) is established. \square

THEOREM 3.3. *Suppose $\gamma(\mathbf{n})$ satisfies the energy stable condition (1.5). Then there exists a function $K(\mathbf{n}) < \infty$ only depending on $\gamma(\mathbf{n})$ given by*

$$(3.10) \quad K := K(\mathbf{n}) = \frac{6|\xi|^2 + 8\gamma(\mathbf{n})|\xi| + 16C_1}{\gamma(\mathbf{n})} < \infty, \quad \mathbf{n} \in \mathbb{S}^2,$$

such that $F_K(\mathbf{n}, \mathbf{u}, \mathbf{v}) \geq \gamma^2(\mathbf{u} \times \mathbf{v})$ for any $\mathbf{u}, \mathbf{v} \in \mathbb{S}^2$.

Proof. It is convenient to first consider the special case $\mathbf{n} = (0, 0, 1)^T$. For any $\mathbf{u}, \mathbf{v} \in \mathbb{S}^2$, we write them in the spherical coordinates as

$$(3.11a) \quad \mathbf{u} = (\cos \theta_1 \cos \phi_1, \sin \theta_1 \cos \phi_1, \sin \phi_1)^T, \quad 0 \leq \theta_1 < 2\pi, \quad -\frac{\pi}{2} \leq \phi_1 \leq \frac{\pi}{2},$$

$$(3.11b) \quad \mathbf{v} = (\cos \theta_2 \cos \phi_2, \sin \theta_2 \cos \phi_2, \sin \phi_2)^T, \quad 0 \leq \theta_2 < 2\pi, \quad -\frac{\pi}{2} \leq \phi_2 \leq \frac{\pi}{2},$$

where in case when $\phi_1 = \pm\frac{\pi}{2}$, we choose $\theta_1 = 0$; and when $\phi_2 = \pm\frac{\pi}{2}$, we choose $\theta_2 = 0$. The cross product $\mathbf{u} \times \mathbf{v}$ is then represented as

$$(3.12) \quad \mathbf{u} \times \mathbf{v} = \cos \phi_2 \sin \phi_1 \hat{\mathbf{v}}_0 + \cos \phi_1 \sin \phi_2 \hat{\mathbf{u}}_0 + \cos \phi_1 \cos \phi_2 \hat{\mathbf{w}}_0,$$

where

$$\begin{aligned} \hat{\mathbf{u}}_0 &= (\sin \theta_1, -\cos \theta_1, 0)^T, & \hat{\mathbf{v}}_0 &= (-\sin \theta_2, \cos \theta_2, 0)^T, \\ \hat{\mathbf{w}}_0 &= (0, 0, \sin \theta_{21})^T, & \text{with } \theta_{21} &= \theta_2 - \theta_1. \end{aligned}$$

Since \mathbf{u}, \mathbf{v} are symmetric in $F_K(\mathbf{n}, \mathbf{u}, \mathbf{v})$ and $\gamma^2(\mathbf{u} \times \mathbf{v})$. Without loss of generality, we can always assume $\sin \theta_{21} \geq 0$.

Denoting $\mathbf{u}_0, \mathbf{v}_0 \in \mathbb{S}^2$ as

$$(3.13) \quad \mathbf{u}_0 := (\cos \theta_1, \sin \theta_1, 0)^T, \quad \mathbf{v}_0 := (\cos \theta_2, \sin \theta_2, 0)^T,$$

we know that $|(\mathbf{u} - \mathbf{u}_0) \times \mathbf{v}| \leq |\mathbf{u} - \mathbf{u}_0|, |\mathbf{u} \times (\mathbf{v} - \mathbf{v}_0)| \leq |\mathbf{v} - \mathbf{v}_0|, |(\mathbf{u} - \mathbf{u}_0) \times (\mathbf{v} - \mathbf{v}_0)| \leq |\mathbf{u} - \mathbf{u}_0| + |\mathbf{v} - \mathbf{v}_0|$ since $|\mathbf{u}|, |\mathbf{v}|, |\mathbf{u}_0|, |\mathbf{v}_0| = 1$. Thus we get

$$(3.14) \quad |\mathbf{u} \times \mathbf{v} - \mathbf{u}_0 \times \mathbf{v}_0|^2 \leq 8(|\mathbf{u} - \mathbf{u}_0|^2 + |\mathbf{v} - \mathbf{v}_0|^2).$$

Taking $\mathbf{p} = \mathbf{u} \times \mathbf{v}$, $\mathbf{q} = \mathbf{u}_0 \times \mathbf{v}_0$ in (3.7), and noticing $\mathbf{u}_0 \times \mathbf{v}_0 = (\sin \theta_{21}) \mathbf{n}$, we obtain

$$\begin{aligned}
& \gamma^2(\mathbf{u} \times \mathbf{v}) - (\sin \theta_{21})^2 \gamma^2(\mathbf{n}) \\
& \leq \sin \theta_{21} \nabla(\gamma^2(\mathbf{n})) \cdot (\mathbf{u} \times \mathbf{v} - \mathbf{u}_0 \times \mathbf{v}_0) + C_1 |\mathbf{u} \times \mathbf{v} - \mathbf{u}_0 \times \mathbf{v}_0|^2 \\
& \leq 2\gamma(\mathbf{n}) \boldsymbol{\xi} \cdot (\sin \phi_1 \hat{\mathbf{v}}_0 + \sin \phi_2 \hat{\mathbf{u}}_0) \sin \theta_{21} \\
& \quad + 2\gamma(\mathbf{n}) \boldsymbol{\xi} \cdot ((\cos \phi_2 - 1) \sin \phi_1 \mathbf{v}_0 + (\cos \phi_1 - 1) \sin \phi_2 \mathbf{u}_0) \sin \theta_{21} \\
& \quad + 2\gamma(\mathbf{n}) \boldsymbol{\xi} \cdot \hat{\omega}_0 (1 - \cos \phi_1 \cos \phi_2) \sin \theta_{21} + 8C_1 (|\mathbf{u} - \mathbf{u}_0|^2 + |\mathbf{v} - \mathbf{v}_0|^2) \\
& \leq 2\gamma(\mathbf{n}) \boldsymbol{\xi} \cdot [(\cos \theta_{21} \mathbf{v}_0 - \mathbf{u}_0) (\mathbf{n} \cdot \mathbf{u}) + (\cos \theta_{21} \mathbf{u}_0 - \mathbf{v}_0) (\mathbf{n} \cdot \mathbf{v})] \\
(3.15) \quad & \quad + 4(\gamma(\mathbf{n}) |\boldsymbol{\xi}| + 4C_1) [(\mathbf{n} \cdot \mathbf{u})^2 + (\mathbf{n} \cdot \mathbf{v})^2].
\end{aligned}$$

Here we use the facts $|\mathbf{u} - \mathbf{u}_0| = 2|\sin \frac{\phi_1}{2}|$, $|\mathbf{v} - \mathbf{v}_0| = 2|\sin \frac{\phi_2}{2}|$, $(\sin \phi)^2 \geq 2(\sin \frac{\phi}{2})^2 = 1 - \cos \phi$ for all $-\frac{\pi}{2} \leq \phi \leq \frac{\pi}{2}$, and $0 \leq 1 - \cos \phi_1 \cos \phi_2 \leq (1 - \cos \phi_1) + (1 - \cos \phi_2)$.

To estimate $G(\mathbf{n}, \mathbf{u}, \mathbf{v})$, we observe the following inequalities

$$\begin{aligned}
(\boldsymbol{\xi} \cdot \mathbf{u})(\mathbf{n} \cdot \mathbf{u}) &= (\boldsymbol{\xi} \cdot \mathbf{u}_0)(\mathbf{n} \cdot \mathbf{u}) + (\boldsymbol{\xi} \cdot (\mathbf{u} - \mathbf{u}_0))(\mathbf{n} \cdot (\mathbf{u} - \mathbf{u}_0)) \\
&\leq (\boldsymbol{\xi} \cdot \mathbf{u}_0)(\mathbf{n} \cdot \mathbf{u}) + |\boldsymbol{\xi}| |\mathbf{u} - \mathbf{u}_0|^2 \\
(3.16a) \quad &\leq (\boldsymbol{\xi} \cdot \mathbf{u}_0)(\mathbf{n} \cdot \mathbf{u}) + 2|\boldsymbol{\xi}| (\mathbf{n} \cdot \mathbf{u})^2,
\end{aligned}$$

$$(3.16b) \quad (\boldsymbol{\xi} \cdot \mathbf{v})(\mathbf{n} \cdot \mathbf{v}) \leq (\boldsymbol{\xi} \cdot \mathbf{v}_0)(\mathbf{n} \cdot \mathbf{v}) + 2|\boldsymbol{\xi}| (\mathbf{n} \cdot \mathbf{v})^2.$$

Combining (3.4) and (3.16) yields

$$\begin{aligned}
G(\mathbf{n}, \mathbf{u}, \mathbf{v}) &= \gamma^2(\mathbf{n}) - 2\gamma(\mathbf{n}) [(\boldsymbol{\xi} \cdot \mathbf{u})(\mathbf{n} \cdot \mathbf{u}) + (\boldsymbol{\xi} \cdot \mathbf{v})(\mathbf{n} \cdot \mathbf{v})] \\
(3.17) \quad &\geq \gamma^2(\mathbf{n}) - 2\gamma(\mathbf{n}) [(\boldsymbol{\xi} \cdot \mathbf{u}_0)(\mathbf{n} \cdot \mathbf{u}) + (\boldsymbol{\xi} \cdot \mathbf{u}_0)(\mathbf{n} \cdot \mathbf{u})] \\
&\quad - 4\gamma(\mathbf{n}) |\boldsymbol{\xi}| [(\mathbf{n} \cdot \mathbf{u})^2 + (\mathbf{n} \cdot \mathbf{v})^2].
\end{aligned}$$

Finally, by (3.5) in lemma 3.1, the estimation of $\gamma^2(\mathbf{u} \times \mathbf{v})$ in (3.15), and the estimation of $G(\mathbf{n}, \mathbf{u}, \mathbf{v})$ in (3.17), we obtain

$$\begin{aligned}
& F_K(\mathbf{n}, \mathbf{u}, \mathbf{v}) - \gamma^2(\mathbf{u} \times \mathbf{v}) \\
& \geq \gamma(\mathbf{n})^2 (\cos \theta_{21})^2 - 2\gamma(\mathbf{n}) \cos \theta_{21} [(\boldsymbol{\xi} \cdot \mathbf{v}_0)(\mathbf{n} \cdot \mathbf{u}) + (\boldsymbol{\xi} \cdot \mathbf{u}_0)(\mathbf{n} \cdot \mathbf{v})] \\
& \quad + [\gamma(\mathbf{n}) K(\mathbf{n}) - 4|\boldsymbol{\xi}|^2 - 8\gamma(\mathbf{n}) |\boldsymbol{\xi}| - 16C_1] [(\mathbf{n} \cdot \mathbf{u})^2 + (\mathbf{n} \cdot \mathbf{v})^2] \\
& \geq \gamma(\mathbf{n})^2 (\cos \theta_{21})^2 - 2\gamma(\mathbf{n}) |\cos \theta_{21}| |\boldsymbol{\xi}| [(\mathbf{n} \cdot \mathbf{u}) + (\mathbf{n} \cdot \mathbf{v})] \\
& \quad + 2|\boldsymbol{\xi}|^2 [(\mathbf{n} \cdot \mathbf{u})^2 + (\mathbf{n} \cdot \mathbf{v})^2] \\
& \geq 0.
\end{aligned}$$

Thus we have $F_K(\mathbf{n}, \mathbf{u}, \mathbf{v}) \geq \gamma^2(\mathbf{u} \times \mathbf{v})$ for the special case $\mathbf{n} = (0, 0, 1)^T$.

Since the constant $K(\mathbf{n})$ only depends on $\gamma(\mathbf{n})$, thus the proof is valid for arbitrary $\mathbf{n} \in \mathbb{S}^2$ via a similar argument. The proof is completed. \square

Theorem 3.3 indicates that the set $\{k(\mathbf{n}) \mid F_k(\mathbf{n}, \mathbf{u}, \mathbf{v}) \geq \gamma^2(\mathbf{u} \times \mathbf{v}), \forall \mathbf{u}, \mathbf{v} \in \mathbb{S}^2\}$ contains at least an element $K(\mathbf{n}) < \infty$, and thus it is not empty. This, together with the fact $k_0(\mathbf{n}) \geq \gamma(\mathbf{n})$, yields the existence of the minimal stabilizing function $k_0(\mathbf{n})$.

COROLLARY 3.4 (existence of the minimal stabilizing function). *Suppose the surface energy $\gamma(\mathbf{n})$ satisfying the energy stable condition (1.5). Then the minimal stabilizing function $k_0(\mathbf{n})$ in (3.2) is well-defined.*

Finally, we point out the minimal stabilizing function $k_0(\mathbf{n})$ is determined by $\gamma(\mathbf{n})$, and thus we can consider the mapping from $\gamma(\mathbf{n})$ to $k_0(\mathbf{n})$. Similar to the result in 2D in [6], the mapping is sub-linear.

THEOREM 3.5 (positive homogeneity and subadditivity). *Let $k_0(\mathbf{n})$, $k_1(\mathbf{n})$ and $k_2(\mathbf{n})$ be the minimal stabilizing functions of $\gamma(\mathbf{n})$, $\gamma_1(\mathbf{n})$ and $\gamma_2(\mathbf{n})$, respectively. Then we have*

- (i) *for any $c > 0$, $ck_0(\mathbf{n})$ is the stabilizing function of $c\gamma(\mathbf{n})$; and*
- (ii) *suppose $\gamma(\mathbf{n}) = \gamma_1(\mathbf{n}) + \gamma_2(\mathbf{n})$, then $k_0(\mathbf{n}) \leq k_1(\mathbf{n}) + k_2(\mathbf{n})$ for $\mathbf{n} \in \mathbb{S}^2$.*

Proof. The proof of positive homogeneity in (i) is similar to the proof of Lemma 4.4 in [6], and thus details are omitted here for brevity.

To prove the subadditivity in (ii), we denote

$$\xi := \nabla \gamma(\mathbf{p})|_{\mathbf{p}=\mathbf{n}}, \quad \xi_1 := \nabla \gamma_1(\mathbf{p})|_{\mathbf{p}=\mathbf{n}}, \quad \xi_2 := \nabla \gamma_2(\mathbf{p})|_{\mathbf{p}=\mathbf{n}}.$$

Since $k_1(\mathbf{n})$ is the minimal stabilizing function of $\gamma_1(\mathbf{n})$, for any $t \in \mathbb{R}$, we have

$$\begin{aligned} & \frac{1}{2} \mathbf{u}^T \mathbf{Z}_{k_1}(\mathbf{n}) \mathbf{u} + \frac{t^2}{2} \mathbf{v}^T \mathbf{Z}_{k_1}(\mathbf{n}) \mathbf{v} - t \gamma_1(\mathbf{u} \times \mathbf{v}) \\ & \geq 2 \sqrt{\frac{t^2}{4} F_{k_1}(\mathbf{n}, \mathbf{u}, \mathbf{v}) - t \gamma_1(\mathbf{u} \times \mathbf{v})} \\ (3.18) \quad & \geq 0, \quad \forall \mathbf{n}, \mathbf{u}, \mathbf{v} \in \mathbb{S}^2. \end{aligned}$$

A similar inequality is also true for $\gamma_2(\mathbf{n})$. Adding the two inequalities together and noticing $\xi = \xi_1 + \xi_2$, we obtain

$$(3.19) \quad \frac{1}{2} \mathbf{u}^T \mathbf{Z}_{k_1+k_2}(\mathbf{n}) \mathbf{u} + \frac{t^2}{2} \mathbf{v}^T \mathbf{Z}_{k_1+k_2}(\mathbf{n}) \mathbf{v} - t \gamma(\mathbf{u} \times \mathbf{v}) \geq 0, \quad \forall t \in \mathbb{R},$$

which means its discriminant $\gamma^2(\mathbf{u} \times \mathbf{v}) - F_{k_1+k_2}(\mathbf{n}, \mathbf{u}, \mathbf{v}) \leq 0$ for all $\mathbf{n}, \mathbf{u}, \mathbf{v} \in \mathbb{S}^2$. Then the subadditivity is a direct conclusion from the definition of the minimal stabilizing function (3.2). \square

3.2. Proof of energy stability in Theorem 2.2. After establishing the existence of the minimal stabilizing function $k_0(\mathbf{n})$, we now have enough tools to prove the unconditionally energy stability (2.24b) in Theorem 2.2. To simplify the proof, we first introduce the following alternative definition of the surface gradient operator ∇_S .

LEMMA 3.6. *Suppose σ be a non-degenerated triangle with three vertices $\{\mathbf{q}_1, \mathbf{q}_2, \mathbf{q}_3\}$ ordered counterclockwise. Let f and \mathbf{F} be scalar- and vector-valued functions in $\mathcal{P}^1(\sigma)/[\mathcal{P}^1(\sigma)]^3$, respectively, $\{\mathbf{n}, \boldsymbol{\tau}_1, \boldsymbol{\tau}_2\}$ forms an orthonormal basis. Then the discretized surface gradient operator ∇_S in (2.20) satisfies*

$$(3.20) \quad \nabla_S f = (\partial_{\boldsymbol{\tau}_1} f) \boldsymbol{\tau}_1 + (\partial_{\boldsymbol{\tau}_2} f) \boldsymbol{\tau}_2, \quad \nabla_S \mathbf{F} = (\partial_{\boldsymbol{\tau}_1} \mathbf{F}) \boldsymbol{\tau}_1^T + (\partial_{\boldsymbol{\tau}_2} \mathbf{F}) \boldsymbol{\tau}_2^T,$$

where $\partial_{\boldsymbol{\tau}} f$ denotes the directional derivative of f with respect to $\boldsymbol{\tau}$.

Proof. It suffices to prove the left equality in (3.20). Let $\mathbf{x} = \lambda_1 \mathbf{q}_1 + \lambda_2 \mathbf{q}_2 + \lambda_3 \mathbf{q}_3$ with $0 \leq \lambda_1, \lambda_2, \lambda_3 \leq 1$ satisfying $\lambda_1 + \lambda_2 + \lambda_3 = 1$ be a point in σ . We observe that

$$\begin{aligned} & [(\mathbf{q}_3 - \mathbf{q}_2) \times \mathbf{n}] \cdot (\mathbf{x} - \mathbf{q}_3) = [(\mathbf{x} - \mathbf{q}_3) \times (\mathbf{q}_3 - \mathbf{q}_2)] \cdot \mathbf{n} \\ & = [(-\lambda_1(\mathbf{q}_3 - \mathbf{q}_1) - \lambda_2(\mathbf{q}_3 - \mathbf{q}_2)) \times (\mathbf{q}_3 - \mathbf{q}_2)] \cdot \mathbf{n} \\ & = -\lambda_1 [(\mathbf{q}_2 - \mathbf{q}_1 + \mathbf{q}_3 - \mathbf{q}_2) \times (\mathbf{q}_3 - \mathbf{q}_2)] \cdot \mathbf{n} \\ (3.21) \quad & = -\lambda_1 |\mathcal{J}\{\sigma\}|. \end{aligned}$$

Thus $\lambda_1 = \frac{(\mathbf{q}_2 - \mathbf{q}_3) \times \mathbf{n}}{|\mathcal{J}\{\sigma\}|} \cdot (\mathbf{x} - \mathbf{q}_3)$, and λ_2, λ_3 can be derived similarly.

By the definition of the directional derivative, we deduce that

$$\begin{aligned}
 \partial_{\tau_1} f(\mathbf{x}) &= \lim_{h \rightarrow 0} \frac{f(\mathbf{x} + h\tau_1) - f(\mathbf{x})}{h} \\
 &= \lim_{h \rightarrow 0} \frac{1}{h} \left(f(\mathbf{q}_1) \frac{(\mathbf{q}_2 - \mathbf{q}_3) \times \mathbf{n}}{|\mathcal{J}\{\sigma\}|} \cdot (h\tau_1) \right. \\
 &\quad \left. + f(\mathbf{q}_2) \frac{(\mathbf{q}_3 - \mathbf{q}_1) \times \mathbf{n}}{|\mathcal{J}\{\sigma\}|} \cdot (h\tau_1) + f(\mathbf{q}_3) \frac{(\mathbf{q}_1 - \mathbf{q}_2) \times \mathbf{n}}{|\mathcal{J}\{\sigma\}|} \cdot (h\tau_1) \right) \\
 (3.22) \quad &= \nabla_S f(\mathbf{x}) \cdot \tau_1.
 \end{aligned}$$

Similarly, we have $\partial_{\tau_2} f = \nabla_S f \cdot \tau_2$. Since $\{\mathbf{n}, \tau_1, \tau_2\}$ forms an orthonormal basis, by vector decomposition and $\nabla_S f \cdot \mathbf{n} = 0$, we obtain

$$\begin{aligned}
 \nabla_S f &= (\nabla_S f \cdot \mathbf{n}) \mathbf{n} + (\nabla_S f \cdot \tau_1) \tau_1 + (\nabla_S f \cdot \tau_2) \tau_2 \\
 (3.23) \quad &= (\partial_{\tau_1} f) \tau_1 + (\partial_{\tau_2} f) \tau_2,
 \end{aligned}$$

which is the desired identity. \square

With the help of (3.20), we can then give the following upper bound of the summand $\gamma(\mathbf{n}) |\sigma|$ in the discretized energy W^m in (2.23b).

LEMMA 3.7. *Suppose σ and $\bar{\sigma}$ are two non-degenerated triangles with counterclockwise ordered vertices $\{\mathbf{q}_1, \mathbf{q}_2, \mathbf{q}_3\}$ and $\{\bar{\mathbf{q}}_1, \bar{\mathbf{q}}_2, \bar{\mathbf{q}}_3\}$, and outward unit normal vectors \mathbf{n} and $\bar{\mathbf{n}}$, respectively. Let \mathbf{X} be a vector-valued function in $[\mathcal{P}^1(\sigma)]^3$ satisfying $\mathbf{X}(\mathbf{q}_i) = \bar{\mathbf{q}}_i$ for $i = 1, 2, 3$. Then for any $k(\mathbf{n}) \geq k_0(\mathbf{n})$ for $\mathbf{n} \in \mathbb{S}^2$, the following inequality holds*

$$(3.24) \quad \frac{1}{6} |\sigma| \sum_{i=1}^3 (\mathbf{Z}_k(\mathbf{n}) \nabla_S \mathbf{X}(\mathbf{q}_i^-)) : \nabla_S \mathbf{X}(\mathbf{q}_i^-) \geq \gamma(\bar{\mathbf{n}}) |\bar{\sigma}|.$$

Proof. Since $\mathbf{X} \in [\mathcal{P}^1(\sigma)]^3$, its derivative $\nabla_S \mathbf{X}$ is a constant matrix in σ . Suppose $\{\mathbf{n}, \tau_1, \tau_2\}$ forms an orthonormal basis, by applying (3.20), we obtain

$$(3.25) \quad \nabla_S \mathbf{X}((\mathbf{q}_i)^-) = (\partial_{\tau_1} \mathbf{X}(\mathbf{q}_i^-)) \tau_1^T + (\partial_{\tau_2} \mathbf{X}(\mathbf{q}_i^-)) \tau_2^T, \quad i = 1, 2, 3.$$

Let $\partial_{\tau_1} \mathbf{X} = s\mathbf{u}$ and $\partial_{\tau_2} \mathbf{X} = t\mathbf{v}$ with $s, t \geq 0$ and $\mathbf{u}, \mathbf{v} \in \mathbb{S}^2$. Substituting this and the definition of $Z_k(\mathbf{n})$ in (2.8) into the LHS of (3.24), we get

$$\begin{aligned}
 &\frac{1}{6} |\sigma| \sum_{i=1}^3 (\mathbf{Z}_k(\mathbf{n}) \nabla_S \mathbf{X}(\mathbf{q}_i^-)) : \nabla_S \mathbf{X}(\mathbf{q}_i^-) \\
 &= \frac{1}{2} |\sigma| (\mathbf{Z}_k(\mathbf{n}) (s\mathbf{u}\tau_1^T + t\mathbf{v}\tau_2^T)) : (s\mathbf{u}\tau_1^T + t\mathbf{v}\tau_2^T) \\
 &= \frac{1}{2} |\sigma| (s^2 (\tau_1 \cdot \tau_1) \mathbf{u}^T \mathbf{Z}_k(\mathbf{n}) \mathbf{u} + t^2 (\tau_2 \cdot \tau_2) \mathbf{v}^T \mathbf{Z}_k(\mathbf{n}) \mathbf{v}) \\
 (3.26) \quad &\geq st |\sigma| \sqrt{F_k(\mathbf{n}, \mathbf{u}, \mathbf{v})} \geq st |\sigma| \gamma(\mathbf{u} \times \mathbf{v}).
 \end{aligned}$$

For the RHS of (3.24), since $\bar{\sigma} = \mathbf{X}(\sigma)$, it holds that

$$(3.27) \quad \gamma(\bar{\mathbf{n}}) |\bar{\sigma}| = \gamma(\bar{\mathbf{n}}) \int_{\sigma} |(\partial_{\tau_1} \mathbf{X}) \times (\partial_{\tau_2} \mathbf{X})| dA = st |\sigma| \gamma(\bar{\mathbf{n}}) |\mathbf{u} \times \mathbf{v}|.$$

Finally, since $\mathbf{X} \in [\mathcal{P}^1(\sigma)]^3$, for \mathbf{p} and $\mathbf{p} + h\boldsymbol{\tau}_1$ in σ , we have $\mathbf{X}(\mathbf{p} + h\boldsymbol{\tau}_1)$ and $\mathbf{X}(\mathbf{p})$ in $\bar{\sigma}$. From the definition of directional derivative for functions in $[\mathcal{P}^1(\sigma)]^3$, we get

$$(3.28) \quad s\mathbf{u} \cdot \bar{\mathbf{n}} = (\partial_{\boldsymbol{\tau}_1} \mathbf{X}) \cdot \bar{\mathbf{n}} = \frac{\mathbf{X}(\mathbf{p} + h\boldsymbol{\tau}_1) - \mathbf{X}(\mathbf{p})}{h} \cdot \bar{\mathbf{n}} = 0,$$

and similarly $\mathbf{v} \cdot \bar{\mathbf{n}} = 0$, thus $\gamma(\mathbf{u} \times \mathbf{v}) = |\mathbf{u} \times \mathbf{v}| \gamma(\bar{\mathbf{n}})$. This equation, together with (3.26) and (3.27), yields the desired inequality (3.24). \square

With the help of Lemma (3.7), we can then prove the unconditional energy stability (2.24b) in the main Theorem 2.2.

Proof. For any fixed $\mathbf{n} \in \mathbb{S}^2$, noting (2.8), we get

$$(3.29) \quad \mathbf{p}^T \mathbf{Z}_k(\mathbf{n}) \mathbf{p} = \gamma(\mathbf{n}) - 2(\boldsymbol{\xi} \cdot \mathbf{p})(\mathbf{n} \cdot \mathbf{p}) + k(\mathbf{n})(\mathbf{n} \cdot \mathbf{p})^2, \quad \forall \mathbf{p} \in \mathbb{S}^2.$$

For $\mathbf{p} \in \mathbb{S}^2$ satisfying $\mathbf{p} \cdot \mathbf{n} = 0$, we get $\mathbf{p}^T \mathbf{Z}_k(\mathbf{n}) \mathbf{p} = \gamma(\mathbf{n}) > 0$. On the other hand, for $\mathbf{p} \in \mathbb{S}^2$ satisfying $\mathbf{p} \cdot \mathbf{n} \neq 0$, taking $\boldsymbol{\tau} \in \mathbb{S}^2$ satisfying $\boldsymbol{\tau} \cdot \mathbf{n} = 0$, then $\mathbf{p} \times \boldsymbol{\tau} \neq \mathbf{0}$. Since $k(\mathbf{n}) \geq k_0(\mathbf{n})$, noting (3.2) and (3.1) with $\mathbf{u} = \mathbf{p}$ and $\mathbf{v} = \boldsymbol{\tau}$, we obtain

$$\mathbf{p}^T \mathbf{Z}_k(\mathbf{n}) \mathbf{p} = \frac{F_k(\mathbf{n}, \mathbf{p}, \boldsymbol{\tau})}{\boldsymbol{\tau}^T \mathbf{Z}_k(\mathbf{n}) \boldsymbol{\tau}} \geq \frac{\gamma^2(\mathbf{p} \times \boldsymbol{\tau})}{\gamma(\mathbf{n})} > 0.$$

Then $\mathbf{p}^T \mathbf{Z}_k(\mathbf{n}) \mathbf{p} > 0$ for all $\mathbf{p} \in \mathbb{S}^2$, and thus $\mathbf{Z}_k(\mathbf{n})$ is a symmetric positive definite matrix when $k(\mathbf{n}) \geq k_0(\mathbf{n})$ for all $\mathbf{n} \in \mathbb{S}^2$. By Cauchy inequality, it holds that

$$(3.30) \quad \begin{aligned} & \langle \mathbf{Z}_k(\mathbf{n}^m) \nabla_S \mathbf{X}^{m+1}, \nabla_S (\mathbf{X}^{m+1} - \mathbf{X}^m) \rangle_{S^m}^h \\ & \geq \frac{1}{2} \langle \mathbf{Z}_k(\mathbf{n}^m) \nabla_S \mathbf{X}^{m+1}, \nabla_S \mathbf{X}^{m+1} \rangle_{S^m}^h - \frac{1}{2} \langle \mathbf{Z}_k(\mathbf{n}^m) \nabla_S \mathbf{X}^m, \nabla_S \mathbf{X}^m \rangle_{S^m}^h. \end{aligned}$$

Suppose $\{\mathbf{n}_j^m, \boldsymbol{\tau}_{j,1}^m, \boldsymbol{\tau}_{j,2}^m\}$ ($1 \leq j \leq J$) forms an orthonormal basis, by using (3.20), we obtain

$$(3.31) \quad \begin{aligned} & \frac{1}{2} \langle \mathbf{Z}_k(\mathbf{n}^m) \nabla_S \mathbf{X}^m, \nabla_S \mathbf{X}^m \rangle_{S^m}^h \\ & = \frac{1}{6} \sum_{j=1}^J \sum_{i=1}^3 |\sigma_j^m| \left(\mathbf{Z}_k(\mathbf{n}_j^m) \nabla_S \mathbf{X}^m ((\mathbf{q}_{j,i}^m)^-) |_{\sigma_j^m} \right) : \left(\nabla_S \mathbf{X}^m ((\mathbf{q}_{j,i}^m)^-) |_{\sigma_j^m} \right) \\ & = \frac{1}{2} \sum_{j=1}^J |\sigma_j^m| [(\boldsymbol{\tau}_{j,1}^m)^T \mathbf{Z}_k(\mathbf{n}_j^m) \boldsymbol{\tau}_{j,1}^m + (\boldsymbol{\tau}_{j,2}^m)^T \mathbf{Z}_k(\mathbf{n}_j^m) \boldsymbol{\tau}_{j,2}^m] \\ & = \frac{1}{2} \sum_{j=1}^J |\sigma_j^m| \gamma(\mathbf{n}_j^m) (\boldsymbol{\tau}_{j,1}^m \cdot \boldsymbol{\tau}_{j,1}^m + \boldsymbol{\tau}_{j,2}^m \cdot \boldsymbol{\tau}_{j,2}^m) \\ & = \sum_{j=1}^J |\sigma_j^m| \gamma(\mathbf{n}_j^m) = W^m. \end{aligned}$$

For $1 \leq j \leq J$, applying Lemma (3.7) with $\sigma = \sigma_j^m, \bar{\sigma} = \sigma_j^{m+1}$ and $\mathbf{X} = \mathbf{X}^{m+1}|_{\sigma_j^m}$, we get

$$(3.32) \quad \frac{1}{6} |\sigma_j^m| \sum_{i=1}^3 \left(\mathbf{Z}_k(\mathbf{n}_j^m) \nabla_S \mathbf{X}(\mathbf{q}_i^-) |_{\sigma_j^m} \right) : \nabla_S \mathbf{X}(\mathbf{q}_i^-) |_{\sigma_j^m} \geq \gamma(\mathbf{n}_j^{m+1}) |\sigma_j^{m+1}|.$$

Summing (3.32) for $j = 1, 2, \dots, J$ and combining (3.30) and (3.31), we obtain

$$(3.33) \quad \langle \mathbf{Z}_k(\mathbf{n}^m) \nabla_S \mathbf{X}^{m+1}, \nabla_S (\mathbf{X}^{m+1} - \mathbf{X}^m) \rangle_{S^m}^h \geq W^{m+1} - W^m, \quad m \geq 0.$$

Finally, choosing $\psi = \mu^{m+1}$ in (2.21a) and $\omega = \mathbf{X}^{m+1}$ in (2.21b), noting (3.33), we have

$$(3.34) \quad W^{m+1} - W^m \leq \tau \langle \nabla_S \mu^{m+1}, \nabla_S \mu^{m+1} \rangle_{S^m}^h \leq 0, \quad m \geq 0,$$

which immediately implies the unconditionally energy stability (2.24b) in Theorem 2.2. \square

4. Numerical results. In this section, we first state the setup for solving the SP-PFEM (2.21). Then we present serval numerical computations, including the convergence test and the structure-preserving test. Finally, we apply (2.21) to simulate surface evolution for different anisotropic energies.

In our practical computations, the minimal stabilizing function $k_0(\mathbf{n})$ can be obtained via numerically solving (3.2). Then by taking a stabilizing function $k(\mathbf{n}) \geq k_0(\mathbf{n})$ for $\mathbf{n} \in \mathbb{S}^2$, we can determine the surface energy matrix $\mathbf{Z}_k(\mathbf{n})$, and thus the SP-PFEM (2.21) is well-determined. At each time step, the nonlinear system (2.21) is solved by the Newton's method with a given tolerance at $\varepsilon_0 = 10^{-12}$ [9].

Given an initial closed surface S_0 , we generate its approximation $S^0 := S_0^h = \cup_{j=1}^J \overline{\sigma_j^0}$ with J triangles $\{\sigma_j^0\}_{j=1}^J$ and I vertices $\{\mathbf{q}_i^0\}_{i=1}^I$ by using the Matlab toolbox called *CFDTool* [36] with a given parameter mesh size h . Given a time step size τ and a mesh size h , we denote $(\mathbf{X}_{h,\tau}^m, \mu_{h,\tau}^m)$ as the solution of (2.21) with the initial approximation S_0^h at the time $t = t_m$. We define $\mathbf{X}_{h,\tau}(t)$ by

$$(4.1) \quad \mathbf{X}_{h,\tau}(\cdot, t) = \frac{t - t_m}{\tau} \mathbf{X}_{h,\tau}^m(\cdot) + \frac{t_{m+1} - t}{\tau} \mathbf{X}_{h,\tau}^{m+1}(\cdot), \quad \forall t \in [t_m, t_{m+1}], \quad m \geq 0,$$

and the surface $S_{h,\tau}(t)$ is represented by $\mathbf{X}_{h,\tau}(\cdot, t)$.

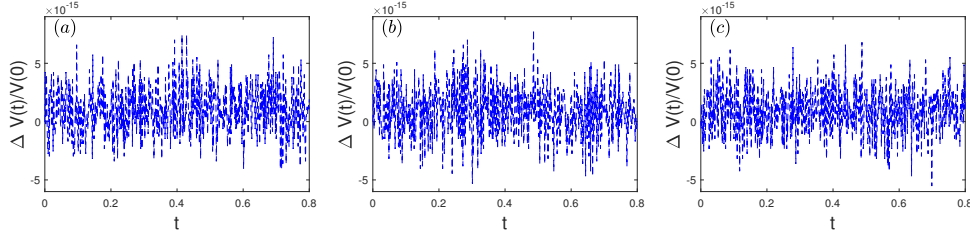


FIG. 4.1. Plot of the normalized volume change $\frac{\Delta V(t)}{V(0)}$ for different cases: (a) for Case 1, (b) for Case 2, and (c) for Case 3.

To test the convergence rate of (2.21), we adopt the manifold distance $M(\cdot, \cdot)$ to measure the difference between two closed surfaces S_1 and S_2 , which is given by

$$(4.2) \quad M(S_1, S_2) := 2|\Omega_1 \cup \Omega_2| - |\Omega_1| - |\Omega_2|,$$

where Ω_1 and Ω_2 are the regions enclosed by S_1 and S_2 , respectively, and $|\Omega|$ denotes the volume of the region Ω . Based on the manifold distance, the numerical error is defined as

$$(4.3) \quad e_{h,\tau}(t) := M(S_{h,\tau}(t), S(t)), \quad t \geq 0.$$

| (h, τ) | $e_{h,\tau}(\frac{1}{2})$ | Case 1 | order | $e_{h,\tau}(\frac{1}{2})$ | Case 2 | order | $e_{h,\tau}(\frac{1}{2})$ | Case 3 | order |
|---|---------------------------|--------|-------|---------------------------|--------|-------|---------------------------|--------|-------|
| (h_0, τ_0) | 1.24E-1 | - | | 1.47E-1 | - | | 1.12E-1 | - | |
| $(\frac{h_0}{2}, \frac{\tau_0}{4})$ | 3.06E-2 | 2.01 | | 3.54E-2 | 2.05 | | 2.82E-2 | 1.98 | |
| $(\frac{h_0}{2^2}, \frac{\tau_0}{4^2})$ | 7.90E-3 | 1.96 | | 8.74E-3 | 2.02 | | 7.54E-3 | 1.90 | |
| (h, τ) | $e_{h,\tau}(\frac{1}{2})$ | Case 4 | order | $e_{h,\tau}(\frac{1}{2})$ | Case 5 | order | $e_{h,\tau}(\frac{1}{2})$ | Case 6 | order |
| (h_0, τ_0) | 1.10E-1 | - | | 1.12E-1 | - | | 1.12E-1 | - | |
| $(\frac{h_0}{2}, \frac{\tau_0}{4})$ | 2.83E-2 | 1.96 | | 2.89E-2 | 1.96 | | 3.09E-2 | 1.99 | |
| $(\frac{h_0}{2^2}, \frac{\tau_0}{4^2})$ | 7.48E-3 | 1.92 | | 7.58E-3 | 1.93 | | 7.86E-3 | 1.97 | |
| (h, τ) | $e_{h,\tau}(1)$ | Case 1 | order | $e_{h,\tau}(1)$ | Case 2 | order | $e_{h,\tau}(1)$ | Case 3 | order |
| (h_0, τ_0) | 1.46E-1 | - | | 1.22E-1 | - | | 1.11E-1 | - | |
| $(\frac{h_0}{2}, \frac{\tau_0}{4})$ | 3.52E-2 | 2.05 | | 3.01E-2 | 2.02 | | 2.74E-2 | 2.02 | |
| $(\frac{h_0}{2^2}, \frac{\tau_0}{4^2})$ | 8.67E-3 | 2.02 | | 7.75E-3 | 1.96 | | 7.21E-3 | 1.93 | |
| (h, τ) | $e_{h,\tau}(1)$ | Case 4 | order | $e_{h,\tau}(1)$ | Case 5 | order | $e_{h,\tau}(1)$ | Case 6 | order |
| (h_0, τ_0) | 1.10E-1 | - | | 1.10E-1 | - | | 1.13E-1 | - | |
| $(\frac{h_0}{2}, \frac{\tau_0}{4})$ | 2.76E-2 | 1.99 | | 2.80E-2 | 1.97 | | 2.90E-2 | 1.96 | |
| $(\frac{h_0}{2^2}, \frac{\tau_0}{4^2})$ | 7.23E-3 | 1.93 | | 7.36E-3 | 1.93 | | 7.56E-3 | 1.94 | |

TABLE 4.1

Numerical errors of $e_{h,\tau}(t = 0.5)$ and $e_{h,\tau}(t = 1)$ for Cases 1-6, while $h_0 := 2^{-1}$ and $\tau_0 := \frac{2^{-1}}{25}$ with 140 triangles and 72 vertices for the initial partition $S_0^{h_0}$, with 624 triangles and 314 vertices for the initial partition $S_0^{h_0/2}$, and with 2502 triangles and 1253 vertices for the initial partition $S_0^{h_0/4}$.

In our practical computations, $S(t)$ is obtained numerically by taking $k(\mathbf{n}) = k_0(\mathbf{n})$ and with a very refined mesh size at $h = h_e = 2^{-4}$ and a very small time step at $\tau = \tau_e = \frac{2}{25}h_e^2$.

In the numerical experiments for testing convergence rates, the time step size and the mesh size are chosen as $\tau = \frac{2}{25}h^2$, the initial shape S_0 is chosen as a $2 \times 2 \times 1$ cuboid, and its finest partition is a polyhedron $S_0^{h_e}$ with 10718 triangles and 5361 vertices. We consider the following five cases of the anisotropic surface energy $\gamma(\mathbf{n})$ as well as the stabilizing function $k(\mathbf{n})$:

- Case 1: $\gamma(\mathbf{n}) = 1 + \frac{1}{4}(n_1^4 + n_2^4 + n_3^4)$, $k(\mathbf{n}) = k_0(\mathbf{n})$;
- Case 2: $\gamma(\mathbf{n}) = 1 + \frac{1}{2}(n_1^4 + n_2^4 + n_3^4)$, $k(\mathbf{n}) = k_0(\mathbf{n})$;
- Case 3: $\gamma(\mathbf{n}) = (n_1^4 + n_2^4 + n_3^4)^{\frac{1}{4}}$, $k(\mathbf{n}) = k_0(\mathbf{n})$;
- Case 4: $\gamma(\mathbf{n}) = (n_1^4 + n_2^4 + n_3^4)^{\frac{1}{4}}$, $k(\mathbf{n}) = k_0(\mathbf{n}) + 1$;
- Case 5: $\gamma(\mathbf{n}) = (n_1^4 + n_2^4 + n_3^4)^{\frac{1}{4}}$, $k(\mathbf{n}) = k_0(\mathbf{n}) + 2$;
- Case 6: $\gamma(\mathbf{n}) = (n_1^4 + n_2^4 + n_3^4)^{\frac{1}{4}}$, $k(\mathbf{n}) = k_0(\mathbf{n}) + 5$.

The numerical errors are listed in Table 4. We note that while $\gamma(\mathbf{n})$ and $k(\mathbf{n})$ are chosen different in different cases, the convergence rates for this manifold error are all about second order in h . These results indicate that the proposed SP-PFEM (2.21) has a good robustness in convergence rate, which is in general independent of $\gamma(\mathbf{n})$ and $k(\mathbf{n})$. Thus in practical computations, there is no need to choose $k(\mathbf{n})$ as the minimal stabilizing function $k_0(\mathbf{n})$.

To examine the volume conservation and unconditionally energy dissipation, we consider these two indicators: the normalized volume change $\frac{\Delta V(t)}{V(0)} := \frac{V(t) - V(0)}{V(0)}$ and

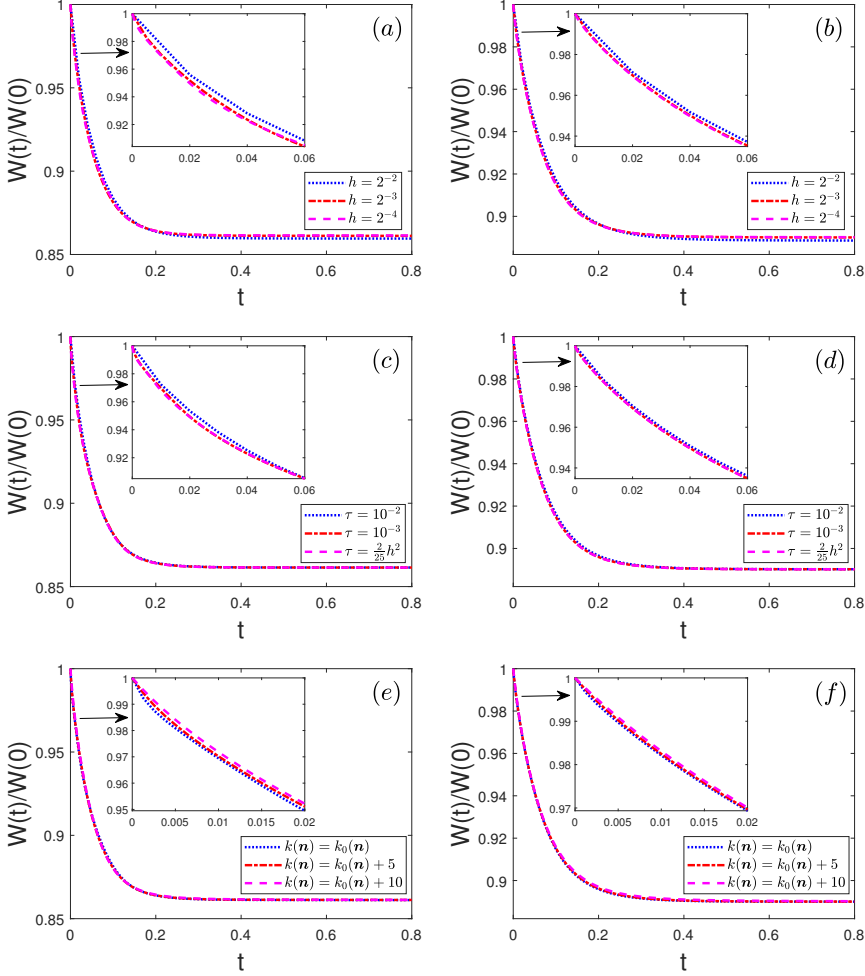


FIG. 4.2. Plot of the normalized energy $\frac{W(t)}{W(0)}$ for weak anisotropy $\gamma(\mathbf{n}) = 1 + \frac{1}{4}(n_1^4 + n_2^4 + n_3^4)$ (left column) and strong anisotropy $\gamma(\mathbf{n}) = 1 + \frac{1}{2}(n_1^4 + n_2^4 + n_3^4)$ (right column) for: with fixed $k(\mathbf{n}) = k_0(\mathbf{n})$ for different h and τ (top row with (a) and (b)), and for fixed $h = 2^{-4}$ and different τ (middle row with (c) and (d)); and with fixed $h = 2^{-4}, \tau = \frac{2}{25}h^2$ for different $k(\mathbf{n})$ (bottom row with (e) and (f)).

the normalized energy $\frac{W(t)}{W(0)}$. The initial shape is taken as a $2 \times 2 \times 1$ ellipsoid. Figure 4.1 shows the normalized volume change $\frac{\Delta V(t)}{V(0)}$ for Cases 1–3 with fixed $h = 2^{-3}$ and $\tau = \frac{2}{25}h^2$. We find the order of magnitude of the volume change $\Delta V(t)$ is at around 10^{-15} , which is close to the machine epsilon at around 10^{-16} , and thus it confirms numerically volume conservation of the SP-PFEM in Theorem (2.2). Figure 4.2 plots the normalized energy $\frac{W(t)}{W(0)}$ for different mesh size h with $\tau = \frac{2}{25}h^2$ and for different τ with a fixed mesh size $h = 2^{-4}$. We observe that the normalized energy $\frac{W(t)}{W(0)}$ is monotonically decreasing in time for all cases, which again confirms the unconditional energy stability of the SP-PFEM in Theorem (2.2). Furthermore, our numerical results suggest that different stabilizing functions $k(\mathbf{n})$ do not pollute

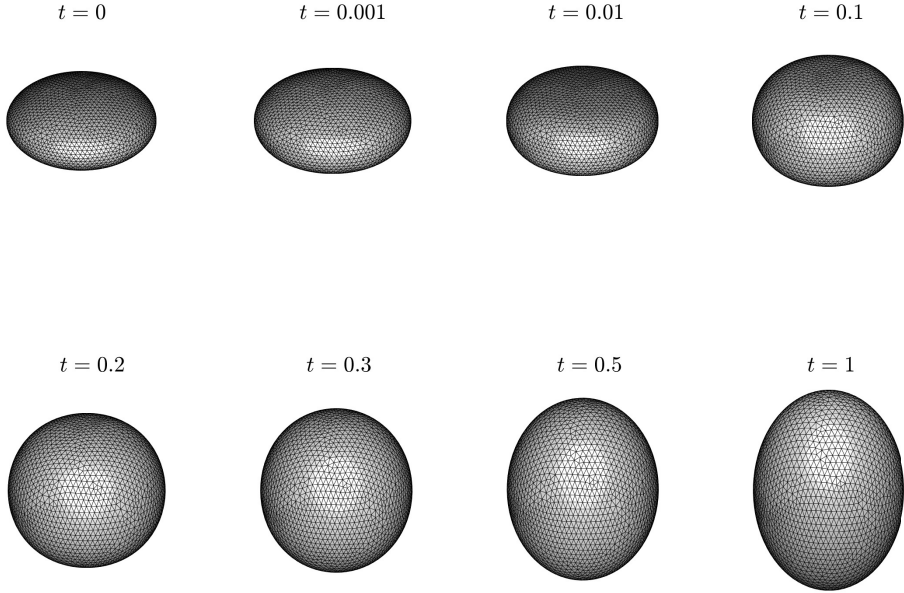


FIG. 4.3. *Evolution of a $2 \times 2 \times 1$ ellipsoid by anisotropic surface diffusion with a weak anisotropy $\gamma(\mathbf{n}) = \sqrt{n_1^2 + n_2^2 + 2n_3^2}$ and $k(\mathbf{n}) = k_0(\mathbf{n})$ at different times.*

the energy too much, and thus we can choose a relatively large stabilizing function $k(\mathbf{n})$ in practical computations.

Finally, we use the SP-PFEM (2.21) to investigate the motion by anisotropic surface diffusion with different anisotropies. We consider the weak anisotropy $\gamma(\mathbf{n}) = \sqrt{n_1^2 + n_2^2 + 2n_3^2}$ with $k(\mathbf{n}) = k_0(\mathbf{n})$. The evolutions of a smooth $2 \times 2 \times 1$ ellipsoid and a non-smooth $2 \times 2 \times 1$ cuboid are shown in figure 4.3 and figure 4.4, respectively. We choose the mesh size $h = 2^{-4}$ and the time step size $\tau = \frac{2}{25}h^2$, and the ellipsoid and the cuboid are initially approximated by 10718 triangles and 5361 vertices, and 32768 triangles and 16386 vertices, respectively. By comparing the two figures, we find the two numerical equilibria are close in shape, which indicates our SP-PFEM (2.21) is robust in capturing the equilibrium shape for different initial shapes. We can see that the meshes are well distributed during the evolution, and there is no need to re-mesh during the evolution.

Then we show the evolution of a strong anisotropy $\gamma(\mathbf{n}) = 1 + \frac{1}{2}(n_1^4 + n_2^4 + n_3^4)$ from a $2 \times 2 \times 1$ cuboid, and the parameters are chosen the same as in previous weak anisotropy. As it can be seen from Figure 4.5, the large and flat facets may be broken into small facets, and the small facets may also merge into a large facet. Moreover, we note from Figure 4.5 that the triangulations become dense at the edges where the facets merge but become sparse at the other edges and at the interior of the facets where the weighted mean curvature μ is almost a constant.

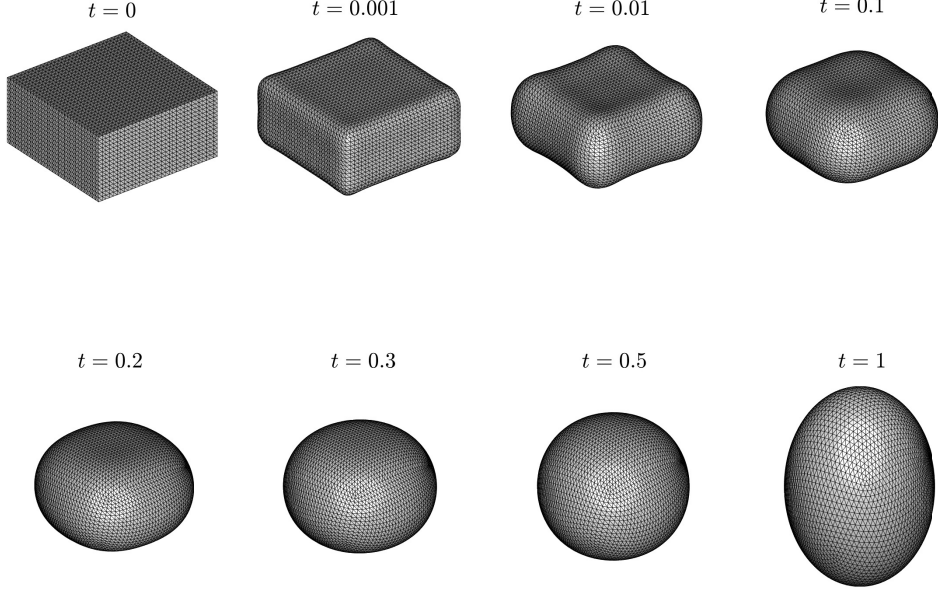


FIG. 4.4. *Evolution of a $2 \times 2 \times 1$ cuboid by anisotropic surface diffusion with a weak anisotropy $\gamma(\mathbf{n}) = \sqrt{n_1^2 + n_2^2 + 2n_3^2}$ and $k(\mathbf{n}) = k_0(\mathbf{n})$ at different times.*

5. Conclusions. By generalizing the symmetrized surface energy matrix $Z_k(\mathbf{n})$ in two dimensions proposed in [6] to three dimensions (3D), which depends on the Cahn-Hoffman ξ -vector and a stabilizing function $k(\mathbf{n})$, we derived a symmetrized and conservative variational formulation for anisotropic surface diffusion with an anisotropic surface energy $\gamma(\mathbf{n})$. A structure-preserving parametric finite element method (SP-PFEM) was proposed to discretize the variational problem, which preserves the volume in the fully discretized level. Under the simple and mild condition (1.5) on $\gamma(\mathbf{n})$ for both weak and strong surface energy anisotropy, we showed that the SP-PFEM is unconditionally energy stable when the stabilizing function $k(\mathbf{n})$ satisfies $k(\mathbf{n}) \geq k_0(\mathbf{n})$ with $k_0(\mathbf{n})$ being the minimal stabilizing function. Numerical examples were presented to demonstrate the efficiency and accuracy as well as mesh robustness of the proposed SP-PFEM for simulating anisotropic surface diffusion. Finally, we point out that the symmetrized surface energy matrix $Z_k(\mathbf{n})$ can be adapted to derive symmetrized and conservative variational formulations for other geometric flows with anisotropic surface energy $\gamma(\mathbf{n})$, such as the anisotropic mean curvature flow [11], the Stefan problem [14], and the anisotropic elastic flow [16].

Appendix A. The Cahn-Hoffman ξ -vectors for several anisotropic surface energies

(i) For the ellipsoidal anisotropic surface energy [11]

$$(A.1) \quad \gamma(\mathbf{n}) = \sqrt{\mathbf{n}^T \mathbf{G} \mathbf{n}}, \quad \mathbf{n} \in \mathbb{S}^2,$$

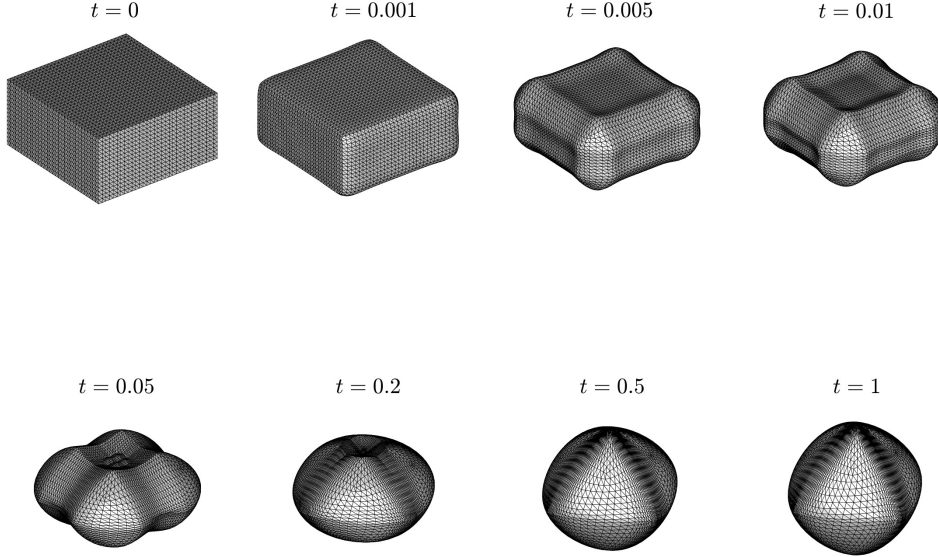


FIG. 4.5. Evolution of a $2 \times 2 \times 1$ cuboid by anisotropic surface diffusion with a strong anisotropy $\gamma(\mathbf{n}) = 1 + \frac{1}{2}(n_1^4 + n_2^4 + n_3^4)$ and $k(\mathbf{n}) = k_0(\mathbf{n})$ at different times.

where $\mathbf{G} \in \mathbb{R}^{3 \times 3}$ is a symmetric positive definite matrix, we have

$$(A.2) \quad \gamma(\mathbf{p}) = \sqrt{\mathbf{p}^T \mathbf{G} \mathbf{p}}, \quad \forall \mathbf{p} \in \mathbb{R}_*^3 := \mathbb{R}^3 \setminus \{\mathbf{0}\},$$

$$(A.3) \quad \boldsymbol{\xi} = \boldsymbol{\xi}(\mathbf{n}) = \gamma(\mathbf{n})^{-1} \mathbf{G} \mathbf{n}, \quad \forall \mathbf{n} \in \mathbb{S}^2,$$

$$(A.4) \quad \mathbf{H}_\gamma(\mathbf{n}) = \gamma(\mathbf{n})^{-3/2} [\gamma(\mathbf{n})^2 \mathbf{G} - (\mathbf{G} \mathbf{n})(\mathbf{G} \mathbf{n})^T].$$

It is easy to check that $\mathbf{H}_\gamma(\mathbf{n})$ is semi-positive definite by using the Cauchy inequality, which indicates the ellipsoidal anisotropy is weakly anisotropic.

(ii) For the l^r -norm ($r \geq 2$) metric anisotropic surface energy [6]

$$(A.5) \quad \gamma(\mathbf{n}) = (|n_1|^r + |n_2|^r + |n_3|^r)^{1/r}, \quad \mathbf{n} = (n_1, n_2, n_3)^T \in \mathbb{S}^2,$$

we have

$$(A.6) \quad \gamma(\mathbf{p}) = \|\mathbf{p}\|_{l^r} = (|p_1|^r + |p_2|^r + |p_3|^r)^{\frac{1}{r}}, \quad \forall \mathbf{p} = (p_1, p_2, p_3)^T \in \mathbb{R}_*^3,$$

$$(A.7) \quad \boldsymbol{\xi} = \boldsymbol{\xi}(\mathbf{n}) = \gamma(\mathbf{n})^{1-r} \begin{pmatrix} |n_1|^{r-2} n_1 \\ |n_2|^{r-2} n_2 \\ |n_3|^{r-2} n_3 \end{pmatrix}, \quad \forall \mathbf{n} = (n_1, n_2, n_3)^T \in \mathbb{S}^2,$$

$$(A.8) \quad \mathbf{H}_\gamma(\mathbf{n}) = (r-1)\gamma(\mathbf{n})^{1-2r} \begin{pmatrix} |n_1|^{r-2}(|n_2|^r + |n_3|^r) & * & * \\ -|n_1 n_2|^{r-2} n_1 n_2 & * & * \\ -|n_1 n_3|^{r-2} n_1 n_3 & * & * \end{pmatrix},$$

where the $*$ entries can be deduced from other entries. By checking leading principal minors, we know that $\mathbf{H}_\gamma(\mathbf{n})$ is semi-positive definite. Thus the l^r -norm anisotropy is weakly anisotropic.

(iii) For the 4-fold anisotropic surface energy [21]

$$(A.9) \quad \gamma(\mathbf{n}) = 1 + \beta(n_1^4 + n_2^4 + n_3^4), \quad \mathbf{n} = (n_1, n_2, n_3)^T \in \mathbb{S}^2,$$

where $\beta > -1$ is a given constant, we have

$$(A.10) \quad \gamma(\mathbf{p}) = (p_1^2 + p_2^2 + p_3^2)^{\frac{1}{2}} + \beta(p_1^4 + p_2^4 + p_3^4)(p_1^2 + p_2^2 + p_3^2)^{-\frac{3}{2}},$$

$$(A.11) \quad \boldsymbol{\xi} = \boldsymbol{\xi}(\mathbf{n}) = \mathbf{n} + \beta(4n_1^3 - 3n_1(n_1^4 + n_2^4 + n_3^4), *, *)^T,$$

$$(A.12) \quad \lambda_1(\mathbf{n}) + \lambda_2(\mathbf{n}) = 2(1 - 3\beta) + 36\beta(n_1^2 n_2^2 + n_2^2 n_3^2 + n_3^2 n_1^2),$$

$$(A.13) \quad \lambda_1(\mathbf{n})\lambda_2(\mathbf{n}) = 20(n_1^4 n_2^4 + n_2^4 n_3^4 + n_3^4 n_1^4) + 72n_1^2 n_2^2 n_3^2 \geq 0.$$

Thus when $\beta = 0$, it is isotropic; when $-1 < \beta < 0$ or $0 < \beta \leq \frac{1}{3}$, it is weakly anisotropic; and when $\beta > \frac{1}{3}$, it is strongly anisotropic.

(iv) Finally, for the regularized BGN anisotropic surface energy [13]

$$(A.14) \quad \gamma(\mathbf{n}) = \left(\sum_{l=1}^L (\mathbf{n}^T \mathbf{G}_l \mathbf{n})^{r/2} \right)^{1/r},$$

where $r \geq 1$ and $\mathbf{G}_1, \mathbf{G}_2, \dots, \mathbf{G}_L$ are symmetric positive definite matrices, we get

$$(A.15) \quad \gamma(\mathbf{p}) = \left(\sum_{l=1}^L (\mathbf{p}^T \mathbf{G}_l \mathbf{p})^{r/2} \right)^{1/r}, \quad \forall \mathbf{p} \in \mathbb{R}_*^3,$$

$$(A.16) \quad \boldsymbol{\xi} = \boldsymbol{\xi}(\mathbf{n}) = \gamma(\mathbf{n})^{1-r} \sum_{l=1}^L \gamma_l^{r-2}(\mathbf{n}) \mathbf{G}_l \mathbf{n} \quad \forall \mathbf{n} \in \mathbb{S}^1,$$

$$(A.17) \quad \mathbf{H}_\gamma(\mathbf{n}) = \gamma(\mathbf{n})^{1-2r} (\mathbf{M}_1 + (r-1)\mathbf{M}_2).$$

where $\gamma_l(\mathbf{n}) := \sqrt{\mathbf{n}^T \mathbf{G}_l \mathbf{n}}$ for $l = 1, 2, \dots, L$, and

$$\begin{aligned} \mathbf{M}_1 &= \gamma(\mathbf{n})^r \sum_{l=1}^L \gamma_l(\mathbf{n})^{r-4} (\gamma_l(\mathbf{n})^2 \mathbf{G}_l - (\mathbf{G}_l \mathbf{n})(\mathbf{G}_l \mathbf{n})^T), \\ \mathbf{M}_2 &= \gamma(\mathbf{n})^r \sum_{l=1}^L (\mathbf{G}_l \mathbf{n})(\mathbf{G}_l \mathbf{n})^T \gamma_l^{r-4}(\mathbf{n}) - \left(\sum_{l=1}^L \gamma_l^{r-2}(\mathbf{n}) \mathbf{G}_l \mathbf{n} \right) \left(\sum_{l=1}^L \gamma_l^{r-2}(\mathbf{n}) \mathbf{G}_l \mathbf{n} \right)^T. \end{aligned}$$

By the Cauchy inequality, we obtain that \mathbf{M}_1 and \mathbf{M}_2 are semi-positive definite. Thus the BGN anisotropy is weakly anisotropic when $r \geq 1$.

REFERENCES

- [1] L. ARMELAO, D. BARRECA, G. BOTTARO, A. GASPAROTTO, S. GROSS, C. MARAGNO, AND E. TONDELLO, *Recent trends on nanocomposites based on cu, ag and au clusters: A closer look*, *Coord. Chem. Rev.*, 250 (2006), pp. 1294–1314.
- [2] R. ASARO AND W. TILLER, *Interface morphology development during stress corrosion cracking: Part i. via surface diffusion*, *Metall. Mater. Trans. B*, 3 (1972), pp. 1789–1796.

- [3] E. BÄNSCH, P. MORIN, AND R. H. NOCHETTO, *Surface diffusion of graphs: variational formulation, error analysis, and simulation*, SIAM J. Numer. Anal., 42 (2004), pp. 773–799.
- [4] W. BAO, H. GARCKE, R. NÜRNBERG, AND Q. ZHAO, *A structure-preserving finite element approximation of surface diffusion for curve networks and surface clusters*, arXiv preprint arXiv:2202.06775, (2022).
- [5] W. BAO, H. GARCKE, R. NÜRNBERG, AND Q. ZHAO, *Volume-preserving parametric finite element methods for axisymmetric geometric evolution equations*, J. Comput. Phys., 460 (2022), p. 111180.
- [6] W. BAO, W. JIANG, AND Y. LI, *A symmetrized parametric finite element method for anisotropic surface diffusion of closed curves via a cahn-hoffman ξ -vector formulation*, arXiv preprint arXiv:2112.00508, (2021).
- [7] W. BAO, W. JIANG, Y. WANG, AND Q. ZHAO, *A parametric finite element method for solid-state dewetting problems with anisotropic surface energies*, J. Comput. Phys., 330 (2017), pp. 380–400.
- [8] W. BAO AND Q. ZHAO, *An energy-stable parametric finite element method for simulating solid-state dewetting problems in three dimensions*, J. Comput. Math., to appear (arXiv: 2012.11404), (2020).
- [9] W. BAO AND Q. ZHAO, *A structure-preserving parametric finite element method for surface diffusion*, SIAM J. Numer. Anal., 59 (2021), pp. 2775–2799.
- [10] J. W. BARRETT, H. GARCKE, AND R. NÜRNBERG, *A parametric finite element method for fourth order geometric evolution equations*, J. Comput. Phys., 222 (2007), pp. 441–467.
- [11] J. W. BARRETT, H. GARCKE, AND R. NÜRNBERG, *Numerical approximation of anisotropic geometric evolution equations in the plane*, IMA J. Numer. Anal., 28 (2008), pp. 292–330.
- [12] J. W. BARRETT, H. GARCKE, AND R. NÜRNBERG, *On the parametric finite element approximation of evolving hypersurfaces in \mathbb{R}^3* , J. Comput. Phys., 227 (2008), pp. 4281–4307.
- [13] J. W. BARRETT, H. GARCKE, AND R. NÜRNBERG, *A variational formulation of anisotropic geometric evolution equations in higher dimensions*, Numer. Math., 109 (2008), pp. 1–44.
- [14] J. W. BARRETT, H. GARCKE, AND R. NÜRNBERG, *On stable parametric finite element methods for the stefan problem and the mullins–sekerka problem with applications to dendritic growth*, J. Comput. Phys., 229 (2010), pp. 6270–6299.
- [15] J. W. BARRETT, H. GARCKE, AND R. NÜRNBERG, *Numerical computations of faceted pattern formation in snow crystal growth*, Phys. Rev. E, 86 (2012), p. 011604.
- [16] J. W. BARRETT, H. GARCKE, AND R. NÜRNBERG, *Parametric approximation of isotropic and anisotropic elastic flow for closed and open curves*, Numer. Math., 120 (2012), pp. 489–542.
- [17] J. W. BARRETT, H. GARCKE, AND R. NÜRNBERG, *Parametric finite element approximations of curvature-driven interface evolutions*, in Handb. Numer. Anal., vol. 21, Elsevier, 2020, pp. 275–423.
- [18] J. W. CAHN AND J. E. TAYLOR, *Overview no. 113 surface motion by surface diffusion*, Acta Metall. Mater., 42 (1994), pp. 1045–1063.
- [19] L.-S. CHANG, E. RABKIN, B. STRAUMAL, B. BARETZKY, AND W. GUST, *Thermodynamic aspects of the grain boundary segregation in cu (bi) alloys*, Acta Mater., 47 (1999), pp. 4041–4046.
- [20] U. CLARENZ, U. DIEWALD, AND M. RUMPF, *Anisotropic geometric diffusion in surface processing*, IEEE Proc. Vis., 2000.
- [21] K. DECKELNICK, G. DZIUK, AND C. M. ELLIOTT, *Computation of geometric partial differential equations and mean curvature flow*, Acta Numer., 14 (2005), pp. 139–232.
- [22] P. DU, M. KHENNER, AND H. WONG, *A tangent-plane marker-particle method for the computation of three-dimensional solid surfaces evolving by surface diffusion on a substrate*, J. Comput. Phys., 229 (2010), pp. 813–827.
- [23] I. FONSECA, A. PRATELLI, AND B. ZWICKNAGL, *Shapes of epitaxially grown quantum dots*, Arch. Ration. Mech. Anal., 214 (2014), pp. 359–401.
- [24] Y. GIGA, *Surface Evolution Equations*, Springer, 2006.
- [25] M. E. GURTIN AND M. E. JABBOUR, *Interface evolution in three dimensions with curvature-dependent energy and surface diffusion: Interface-controlled evolution, phase transitions, epitaxial growth of elastic films*, Arch. Ration. Mech. Anal., 163 (2002), pp. 171–208.
- [26] K. HAUFFE, *The application of the theory of semiconductors to problems of heterogeneous catalysis*, in Adv. Catal., vol. 7, Elsevier, 1955, pp. 213–257.
- [27] F. HAUSER AND A. VOIGT, *A discrete scheme for parametric anisotropic surface diffusion*, J. Sci. Comput., 30 (2007), pp. 223–235.
- [28] D. W. HOFFMAN AND J. W. CAHN, *A vector thermodynamics for anisotropic surfaces: I. fundamentals and application to plane surface junctions*, Surf. Sci., 31 (1972), pp. 368–388.
- [29] W. JIANG, W. BAO, C. V. THOMPSON, AND D. J. SROLOVITZ, *Phase field approach for simu-*

lating solid-state dewetting problems, *Acta Mater.*, 60 (2012), pp. 5578–5592.

[30] W. JIANG, Y. WANG, Q. ZHAO, D. J. SROLOVITZ, AND W. BAO, *Solid-state dewetting and island morphologies in strongly anisotropic materials*, *Scr. Mater.*, 115 (2016), pp. 123–127.

[31] W. JIANG AND Q. ZHAO, *Sharp-interface approach for simulating solid-state dewetting in two dimensions: A Cahn–Hoffman ξ -vector formulation*, *Phys. D*, 390 (2019), pp. 69–83.

[32] Y. LI AND W. BAO, *An energy-stable parametric finite element method for anisotropic surface diffusion*, *J. Comput. Phys.*, 446 (2021), p. 110658.

[33] Z. LI, H. ZHAO, AND H. GAO, *A numerical study of electro-migration voiding by evolving level set functions on a fixed cartesian grid*, *J. Comput. Phys.*, 152 (1999), pp. 281–304.

[34] W. W. MULLINS, *Theory of thermal grooving*, *J. Appl. Phys.*, 28 (1957), pp. 333–339.

[35] M. NAFFOUTI, R. BACKOFEN, M. SALVALAGLIO, T. BOTTEIN, M. LODARI, A. VOIGT, T. DAVID, A. BENKOUIDER, I. FRAJ, L. FAVRE, A. RONDA, I. BERBEZIER, D. GROSSO, M. ABBAROCHI, AND M. BOLLANI, *Complex dewetting scenarios of ultrathin silicon films for large-scale nanoarchitectures*, *Sci. Adv.*, 3 (2017), p. 1472.

[36] P. SIMULATION, *Cfdtool - matlab cfd simulation gui & toolbox, github*. <https://github.com/precise-simulation/cfdtool/releases/tag/1.8.3>, 2022.

[37] J. E. TAYLOR, *Mean curvature and weighted mean curvature*, *Acta Metall. Mater.*, 40 (1992), pp. 1475–1485.

[38] J. E. TAYLOR, J. W. CAHN, AND C. A. HANDWERKER, *Overview no. 98 i—geometric models of crystal growth*, *Acta. Metal. Mater.*, 40 (1992), pp. 1443–1474.

[39] C. V. THOMPSON, *Solid-state dewetting of thin films*, *Annu. Rev. Mater. Res.*, 42 (2012), pp. 399–434.

[40] Y. WANG, W. JIANG, W. BAO, AND D. J. SROLOVITZ, *Sharp interface model for solid-state dewetting problems with weakly anisotropic surface energies*, *Phys. Rev. B*, 91 (2015), p. 045303.

[41] A. WHEELER, *Cahn–Hoffman ξ -vector and its relation to diffuse interface models of phase transitions*, *J. Stat. Phys.*, 95 (1999), pp. 1245–1280.

[42] L. XIA, A. F. BOWER, Z. SUO, AND C. SHIH, *A finite element analysis of the motion and evolution of voids due to strain and electromigration induced surface diffusion*, *J. Mech. Phys. Solids*, 45 (1997), pp. 1473–1493.

[43] Y. XU AND C.-W. SHU, *Local discontinuous Galerkin method for surface diffusion and Willmore flow of graphs*, *J. Sci. Comput.*, 40 (2009), pp. 375–390.

[44] J. YE AND C. V. THOMPSON, *Mechanisms of complex morphological evolution during solid-state dewetting of single-crystal nickel thin films*, *Appl. Phys. Lett.*, 97 (2010), p. 071904.

[45] Q. ZHAO, W. JIANG, AND W. BAO, *A parametric finite element method for solid-state dewetting problems in three dimensions*, *SIAM J. Sci. Comput.*, 42 (2020), pp. B327–B352.